Electronic supplementary information

Achieving Conformational Control in Room-Temperature Phosphorescence and Thermally Activated Delayed Fluorescence Emitters by Functionalization of the Central Core

Nadzeya A. Kukhta,[a†]* Rongjuan Huang,[b†] Andrei S. Batsanov,[a] Martin R. Bryce,[a] * Fernando B. Dias[b] *

[a]*Department of Chemistry, Durham University, South Road, Durham, DH1 3LE, UK*

[b]*Department of Physics, Durham University, South Road, Durham, DH1 3LE, UK*

Contents **Page**

S1. Synthesis and characterization

S1a. General procedures

All reactions were carried out under an argon atmosphere unless otherwise stated. Starting materials were purchased commercially and were used as received. Solvents were dried using an Innovative Technology solvent purification system and were stored in ampules under argon. TLC analysis was carried out using Merck Silica gel 60 F254 TLC plates and spots were visualized using a TLC lamp emitting at 365, 312 or 254 nm. Silica gel column chromatography was performed using silica gel 60 purchased from Sigma Aldrich. ^{1}H and ^{13}C NMR spectroscopy was carried out on Bruker AV400, Varian VNMRS 500 and 700, and Varian Inova 500 NMR spectrometers. Residual solvent peaks were referenced as described in the literature,[1] and all NMR data was processed in MestReNova V10. Melting points were carried out on a Stuart SMP40 machine with a ramping rate of 4 °C min^{-1}. Videos were replayed manually to accurately determine the melting point. High resolution mass spectrometry was carried out on a Waters LCT Premier XE using ASAP ionization. Samples were analyzed directly as solids using N_2 at 350 °C. Elemental analysis was obtained on an Exeter Analytical E-440 machine.

S1b. Synthesis and characterization

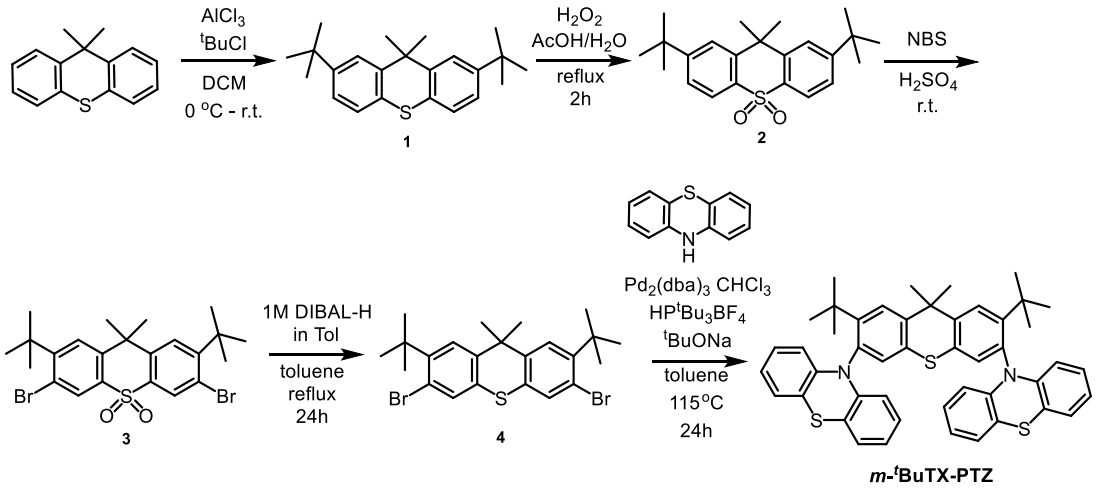

Scheme S1. Synthetic route to ***m*-^{t}BuTX-PTZ**

2,7-Di-*tert*-butyl-9,9-dimethyl-9*H*-thioxanthene (1)

2,7-Di-*tert*-butyl-9,9-dimethyl-9*H*-thioxanthene was prepared according the literature[2] and isolated as a pale yellow waxy solid (3.9 g, yield 95%).

^{1}H NMR (400 MHz, $CDCl_3$) δ: 7.60 (d, 2H, *J* = 2.1 Hz), 7.40 (d, 2H, *J* = 8.1 Hz), 7.26 (td, 2H, *J* = 7.9 Hz, *J* = 2.1 Hz), 1.76 (s, 6H), 1.37 (s, 18H). ^{13}C NMR (101 Hz, $CDCl_3$) δ: 149.6, 142.2, 130.0, 127.0, 123.2, 121.7, 40.9, 34.9, 31.6, 25.3.

2,7-Di-*tert*-butyl-9,9-dimethyl-9*H*-thioxanthene-10,10-dioxide (2)

2,7-Di-*tert*-butyl-9,9-dimethyl-9*H*-thioxanthene-10,10-dioxide was prepared according the procedure described in literature.[3] To a stirring solution of 2,7-di-*tert*-butyl-9,9-dimethyl-9*H*-thioxanthene (**1**) (1.50 g, 4.43 mmol) in AcOH (50 mL) was slowly added H_2O_2 (35 wt% in H_2O, 40 mL). The reaction mixture was refluxed for 2 h and left to cool to room temperature, resulting in the crystallization of pure product, collected by filtration and washed with water and MeOH. White crystalline solid (1.62 g, yield 98%). ^{1}H NMR (400 MHz, $CDCl_3$) δ: 8.14 – 8.10 (m, 2H), 7.76 (d, *J* = 1.7 Hz, 2H), 7.53 (dd, *J* = 8.3, *J* = 1.7 Hz, 2H), 1.92 (s, 6H), 1.38 (s, 18H). ^{3}C NMR (101 Hz, $CDCl_3$) δ: 145.6, 134.1, 124.6, 124.1, 122.3, 39.6, 36.4, 31.2, 30.0.

3,6-Dibromo-2,7-di-*tert*-butyl-9,9-dimethyl-9*H*-thioxanthene-10,10-dioxide (3)

To a stirring solution of 2,7-di-*tert*-butyl-9,9-dimethyl-9*H*-thioxanthene-10,10-dioxide (**2**) (0.80 g, 2.16 mmol) in H_2SO_4 (30 mL) *N*-bromosuccinimide (0.84 g, 4.72 mmol) was added in small portions over the period of 30 min. After being stirred at room temperature for 24 h, the reaction mixture was poured onto crushed ice. The precipitate that formed was filtered and dried in vacuum to afford the product as a yellowish solid (0.61 g, yield 53%).^{1}H NMR (400 MHz, $CDCl_3$) δ: 8.33 (s, 2H), 7.80 (s, 2H), 1.88 (s, 6H), 1.57 (s, 18H). ^{13}C NMR (101 Hz, $CDCl_3$) δ: 153.0, 144.2, 135.2, 131.0, 125.5, 121.5, 39.4, 37.6, 30.7, 29.4. HRMS-ASAP-TOF^{+} m/z calculated for $C_{23}H_{28}Br_2O_2S$ $[M+H]^{+}$ 528.0126, found: 528.0229.

3,6-Dibromo-2,7-di-*tert*-butyl-9,9-dimethyl-9*H*-thioxanthene (4)

Under the argon atmosphere, a solution of DIBAL-H in toluene (1 M, 14.2 mL, 12.8 mmol) was added slowly to a stirring solution of 3,6-dibromo-2,7-di-*tert*-butyl-9,9-dimethyl-9*H*-thioxanthene-10,10-dioxide (**3**) (1.50 g, 2.57 mmol) in toluene (30 mL) at room temperature. After refluxing for 21 h, the reaction mixture was cooled to room temperature and ethanol (1

mL) was cautiously added, followed by H_2O (4 mL) and concentrated HCl (2 mL). The organic layer was separated and washed with brine. The organic layer was dried over $MgSO_4$, filtered and the solvent removed under reduced pressure. After purification by column chromatography (eluent hexane:DCM 5: 1 v/v) and drying in vacuum the product was obtained as a yellowish oil (0.64 g, yield 50%). ^{1}H NMR (400 MHz, acetone-d_6) δ: 7.72 (s, 2H), 7.69 (s, 2H), 1.69 (s, 6H), 1.54 (s, 18H). ^{13}C NMR (101 MHz, acetone-d_6) δ 145.8, 141.2, 133.1, 131.3, 124.7, 119.4, 40.5, 36.6, 30.8, 24.2. HRMS-ASAP-TOF$^+$ m/z calculated for $C_{23}H_{28}Br_2S$ $[M+H]^+$ 494.0278, found: 494.0104.

10,10'-(2,7-di-*tert*-butyl-9,9-dimethyl-9*H*-thioxanthene-3,6-diyl)bis(10*H*-phenothiazine) (*m*-^{t}BuTX-PTZ)

3,6-Dibromo-2,7-di-*tert*-butyl-9,9-dimethyl-9*H*-thioxanthene **4** (0.39 g, 0.78 mmol, 1 eq.) and phenothiazine (0.375 g, 1.88 mmol, 2.4 eq.) were dried under vacuum for 30 min in a two-neck round-bottomed 100 mL flask fitted with a reflux condenser. The flask was back-filled with argon for 30 min, then toluene (25 mL), $Pd_2(dba)_3{\cdot}CHCl_3$ (39 mg, 0.0375 mmol, 0.05 eq.) and HP*t*-Bu_3BF_4 (22 mg, 0.0785 mmol, 0.1 eq.) were added and the reaction mixture was bubbled with argon for 30 min. *t*-BuONa (0.226 g, 2.35 mmol, 3 eq.) was added under a high flow of argon and the reaction was heated then to 115 ^{o}C (DrySyn kit temperature) with stirring for 21 h. After being cooled to room temperature, the reaction mixture was extracted with DCM. Afterwards the organic layer was dried above $MgSO_4$ and filtered. The solvent was removed under reduced pressure and the crude mixture was purified by silica gel chromatography with gradient elution from 15% v/v DCM/hexane switching to 100% CH_2Cl_2 in 10% increasing increments. Removal of solvent under reduced pressure resulted in product as an off-white solid. Recrystallization from DCM/methanol 1/5 v/v gave pale yellow crystals suitable for X-ray analysis (0.10 g, yield 17.5%). ^{1}H NMR (400 Hz, CD_2Cl_2) δ: 7.95 (s, 2H), 7.30 (s, 2H), 7.10 (dd, 4H, *J* = 7.43 Hz, *J* = 1.69 Hz), 6.90-6.93 (m, 4H), 6.86-6.88 (m, 4H), 6.23 (dd, 4H, *J* = 8.10 Hz, *J* = 1.34 Hz), 1.89 (s, 6H), 1.37 (s, 18H). ^{13}C NMR (100 Hz, CD_2Cl_2) δ: 147.8, 146.1, 142.9, 137.0, 133.3, 131.86, 127.1, 127.1, 126.4, 123.0, 120.7, 116.9, 41.6, 36.0, 31.3, 25.6. HRMS-ASAP+ m/z calculated for $C_{47}H_{44}N_2S_3$ [M]+ 733.06, found:733.27. m.p. = 381-383 ^{o}C.

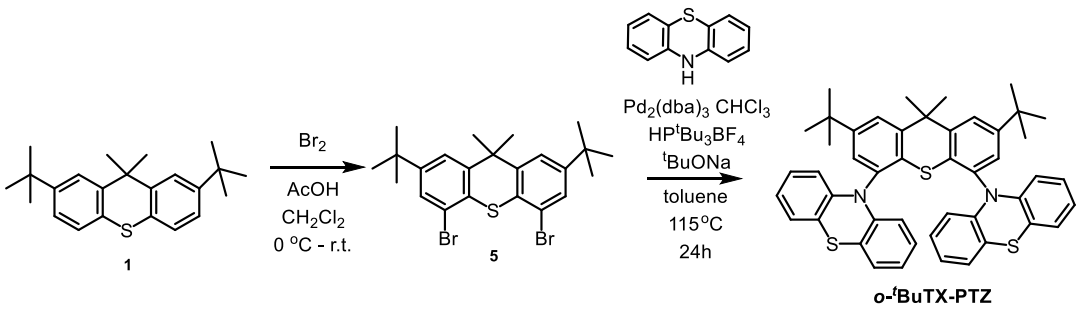

Scheme S2. Synthetic route to ***o*-^{t}BuTX-PTZ**

2,7-Di-*tert*-butyl-4,5-dibromo-9,9-dimethylthioxanthene (5)

2,7-Di-*tert*-butyl-4,5-dibromo-9,9-dimethylthioxanthene was prepared according the literature [2] and isolated as pale pink crystals (2.7 g, yield 92%). ^{1}H NMR (400 MHz, $CDCl_3$) δ: 7.54 (d, 2H, *J* = 1.9 Hz), 7.51 (d, 2H, *J* = 1.9 Hz), 1.70 (s, 6H), 1.35 (s, 18H). ^{13}C NMR (400 MHz, $CDCl_3$) δ: 151.0, 143.3, 130.7, 127.6, 122.2, 120.5, 42.3, 34.9, 31.3, 25.4.

10,10'-(2,7-Di-*tert*-butyl-9,9-dimethyl-9*H*-thioxanthene-4,5-diyl)bis(10*H*-phenothiazine) (*o*-^{t}BuTX-PTZ)

2,7-Di-*tert*-butyl-4,5-dibromo-9,9-dimethylthioxanthene **5** (0.50 g, 1.03 mmol, 1 eq.) and phenothiazine (0.48 g, 2.40 mmol, 2.4 eq.) were dried under vacuum for 30 min in a two-neck round-bottomed 100 mL flask fitted with a reflux condenser. The flask was back-filled with argon for 30 min, then $Pd_2(dba)_3{\cdot}CHCl_3$ (51 mg, 0.05 mmol, 0.05 eq.) and HP*t*-Bu_3BF_4 (29 mg, 0.10 mmol, 0.1 eq.) were added and the reaction mixture was bubbled with argon for 30 min. *t*-BuONa (0.29 g, 3.11 mmol, 3 eq.) was added under a high flow of argon and the reaction was heated then to 115 °C (DrySyn kit temperature) with stirring for 17 h. After being cooled to room temperature, the reaction mixture was extracted with $CHCl_3$. Afterwards the organic layer was dried above $MgSO_4$ and filtered. The solvent was removed under reduced pressure and the crude mixture was purified by silica gel chromatography with gradient elution from 40% v/v $CHCl_3$/hexane switching to 100% $CHCl_3$ in 10% increasing increments. Removal of solvent under reduced pressure resulted in product as a yellow solid. Recrystallization from a boiling mixture of dichloromethane and hexane (1/3 v/v) gave pure product as a white crystalline solid (0.37 g, yield 51%). The crystals were suitable for X-ray analysis. ^{1}H NMR (400 MHz, CD_2Cl_2) δ: 7.72 (d, 2H, *J* = 2.0 Hz), 7.32 (d, 2H, *J* = 1.9 Hz), 6.87 (dd, 4H, *J* = 7.6 Hz, *J* = 1.6 Hz), 6.64

(t, 4H, *J* = 7.6 Hz), 6.58 (dt, 4H, *J* = 7.2 Hz, *J* = 1.5 Hz), 5.94 (dd, 4H, *J* = 8.3 Hz, *J* = 1.2 Hz), 1.76 (s, 6H), 1.38 (s, 18H). ^{13}C NMR (400 MHz, CD_2Cl_2) δ: 151.4, 145.1, 143.1, 137.0, 131.0, 127.5, 126.9, 126.8, 122.8, 121.9, 120.9, 115.3, 41.8, 35.3, 31.6, 25.8. HRMS-ASAP+ m/z calculated for $C_{47}H_{44}N_2S_3$ [M]+ 733.06, found:733.27. Calculated for $C_{47}H_{44}N_2S_3$: C 77.01, H 6.05, N 3.82; found C 77.08, H 6.01, N 3.75. m.p. 373-375 ^{o}C.

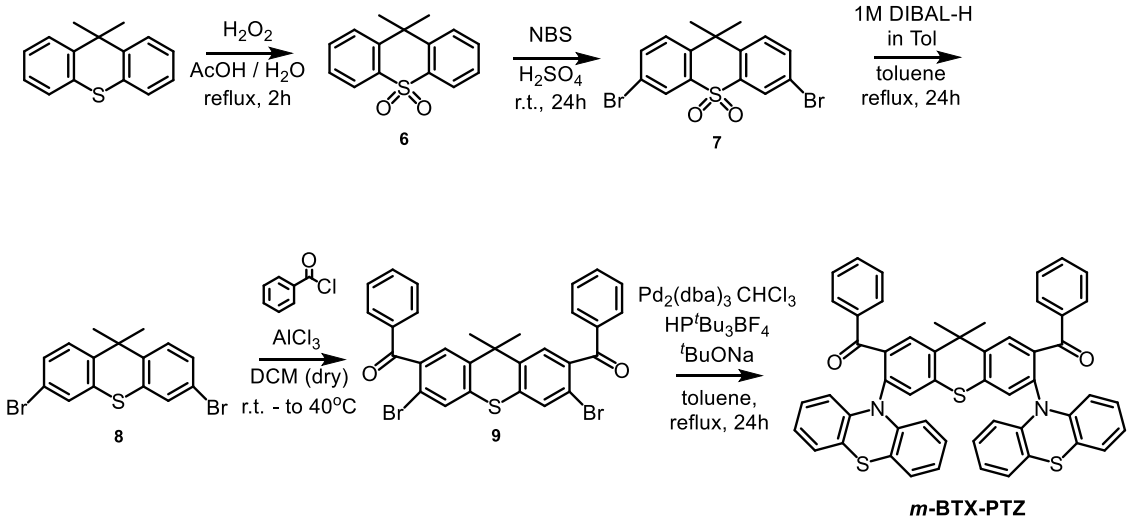

Scheme S3. Synthetic route to ***m*-BTX-PTZ**

9,9-Dimethyl-9H-thioxanthene-10,10-dioxide (6)[3]

To a stirring solution of 9,9-dimethylthioxanthene (2.0 g, 8.98 mmol) in AcOH (60 mL) was slowly added H_2O_2 (35 wt% in H_2O, 50 mL). The reaction mixture was refluxed for 2 h and left to cool to room temperature, resulting in the crystallization of pure product, which was collected by filtration and washed with water and MeOH to give awhite crystalline solid (2.10 g, yield 91%). ^{1}H NMR (400 MHz, $CDCl_3$) δ: 8.22 (dd, 2H, *J* = 7.7 Hz, *J* = 1.5 Hz), 7.77 (dd, 2H, *J* = 8.0 Hz, *J* = 1.1 Hz), 7.62 (td, 2H, *J* = 7.4 Hz, *J* = 1.6 Hz), 7.53 (td, 2H, *J* = 7.6 Hz, *J* = 1.1 Hz), 1.91 (s, 6H). ^{13}C NMR (101 MHz, $CDCl_3$) δ: 145.8, 136.8, 132.8, 127.5, 125.7, 124.3, 39.2, 30.9.

3,6-Dibromo-9,9-dimethyl-9H-thioxanthene-10,10-dioxide (7)[4]

9,9-Dimethylthioxanthene-10,10-dioxide **6** (1.59 g, 5.81 mmol) was dissolved in concentrated H_2SO_4 (35 mL) and *N*-bromosuccinimide (2.06 g, 11.6 mmol) was added slowly over 1 h. The reaction mixture was stirred vigorously for a further 24 h at room temperature. After that, the reaction mixture was poured over ice, resulting in a white precipitate. The resulting solid was recrystallized from ethanol to give white crystals (1.50 g, yield 62%). ^{1}H NMR (400 MHz, $CDCl_3$) δ: 8.31 (d, 2H, *J* = 2.2 Hz), 7.74 (dd, 2H, *J* = 8.6 Hz, *J* = 2.2 Hz), 7.63 (d, 2H, *J* = 8.7 Hz), 1.87 (s, 6H). ^{13}C NMR (101 MHz, $CDCl_3$) δ: 144.2, 137.9, 135.8, 127.5, 127.2, 121.5, 39.1, 30.4.

3,6-Dibromo-9,9-dimethyl-9H-thioxanthene (8)

Under an argon atmosphere, a solution of DIBAL-H in toluene (1 M, 7.2 mL, 7.2 mmol) was slowly added to a stirring solution of 3,6-dibromo-9,9-dimethyl-9*H*-thioxanthene-10,10-dioxide **7** (0.6 g, 1.44 mmol) in toluene (15 mL) at room temperature. After refluxing for 21 h, the reaction mixture was cooled to room temperature and EtOH (1 mL) was cautiously added, followed by H_2O (4 mL) and HCl (2 mL). The organic layer was separated and washed with brine. The organic layer was dried over $MgSO_4$, filtered and the solvent removed under reduced pressure to yield the product as a colorless oil (0.5 g, yield 90%). ^{1}H NMR (400 MHz, CD_2Cl_2) δ: 7.56 (dd, 2H, *J* = 1.8 Hz, *J* = 0.5 Hz), 7.37 (d, 2H, *J* = 1.8 Hz), 7.36 (d, 2H, *J* = 0.5 Hz), 1.63 (s, 6H). ^{13}C NMR (101 MHz, CD_2Cl_2) δ: 141.8, 137.7, 136.0, 127.0, 126.3, 124.5, 40.4, 25.1. HRMS-ASAP-TOF+ m/z calculated for $C_{15}H_{12}Br_2S$ [M+H]+ 381.9026, found: 381.8917.

(3,6-Dibromo-9,9-dimethyl-9*H*-thioxanthene-2,7-diyl)bis(phenylmethanone) (9)

Benzoyl chloride (0.45 mL, 3.9 mmol) was cautiously added dropwise to the solution of 3,6-dibromo-9,9-dimethyl-9*H*-thioxanthene **8** (0.5 g, 1.3 mmol) and $AlCl_3$ (0.52 g, 3.9 mmol) in dry dichloromethane (30 mL) at 0 °C under argon atmosphere. Afterwards the temperature was raised to 40 °C. After being stirred for 24 h at 40 °C, the reaction mixture was cooled to room temperature and extracted with dichloromethane. The organic layer was dried over $MgSO_4$, filtered and the solvent removed under reduced pressure. The crude product was purified by column chromatography using hexane/DCM (1/1 v/v) eluent mixture. After precipitation in

methanol, the product was obtained as the off-white solid (0.43 g, yield 55%). ^{1}H NMR (400 MHz, CD_2Cl_2) δ: 7.80-7.83 (m, 6H), 7.65-7.69 (m, 2H), 7.50-7.54 (m, 6H), 1.68 (s, 6H). ^{13}C NMR (101 MHz, CD_2Cl_2) δ: 195.2, 141.1, 139.1, 136.2, 135.7, 133.8, 131.0, 130.1, 128.7, 125.6, 117.1, 40.3, 24.6. HRMS-ASAP-TOF+ m/z calculated for $C_{29}H_{20}Br_2O_2S$ [M+H]+ 591.9530, found: 591.9001.

(9,9-Dimethyl-3,6-di(10*H*-phenothiazin-10-yl)-9*H*-thioxanthene-2,7-diyl)bis(phenyl-methanone) (*m*-BTX-PTZ)

(3,6-Dibromo-9,9-dimethyl-9*H*-thioxanthene-2,7-diyl)bis(phenylmethanone) **9** (0.10 g, 0.17 mmol, 1 eq.) and phenothiazine (0.074 g, 0.37 mmol, 2.2 eq.) were dried under vacuum for 30 min in a two-neck round-bottomed 100 mL flask fitted with a reflux condenser. The flask was back-filled with argon for 30 min, then toluene (20 mL), $Pd_2(dba)_3{\cdot}CHCl_3$ (8 mg, 0.008 mmol, 0.05 eq.) and $HP^tBu_3BF_4$ (5 mg, 0.016 mmol, 0.1 eq.) were added and the reaction mixture was bubbled with argon for 30 min. ^{t}BuONa (0.048 g, 0.504 mmol, 3 eq.) was added under a high flow of argon and the reaction was heated then to 115 ^{o}C (DrySyn kit temperature) with stirring for 21 h. After being cooled to room temperature, the reaction mixture was extracted with EtOAc. Afterwards the organic layer was dried above $MgSO_4$ and filtered. The solvent was removed under reduced pressure and the crude mixture was purified by silica gel chromatography with gradient elution from 70% v/v DCM/hexane switching to 100% DCM in 10% increasing increments. Removal of solvent under reduced pressure resulted in product as a white solid. Precipitation from DCM to methanol gave a yellow solid (0.11 g, yield 78%). ^{1}H NMR (400 MHz, CD_2Cl_2) δ: 7.93 (s, 2H), 7.75 (s, 2H), 7.58-7.60 (m, 4H), 7.42 (tt, 2H, *J* = 7.4 Hz, *J* = 1.3 Hz), 7.17-7.20 (m, 4H), 6.90 (dd, 2H, *J* = 8.3 Hz, *J* = 1.6 Hz), 6.89 (dd, 2H, *J* = 7.2 Hz, *J* = 1.6 Hz), 6.84 (dd, 4H, *J* = 7.6 Hz, *J* = 1.6 Hz), 6.78 (td, 4H, *J* = 7.4 Hz, *J* = 1.2 Hz), 6.37 (dd, 4H, *J* = 8.2 Hz, *J* = 1.1 Hz), 1.89 (s, 6H). ^{13}C NMR (101 MHz, CD_2Cl_2) δ: 195.9, 143.9, 142.9, 139.4, 137.3, 136.8, 136.6, 133.3, 132.3, 129.9, 128.3, 128.2, 127.0, 126.9, 123.2, 121.21, 116.4, 41.3, 25.4. MALDI-TOF m/z calculated for $C_{53}H_{36}N_2O_2S_3$ [MH]+ 828.19, found:828.1. m.p. = 290-292 ^{o}C.

S1c. ^{1}H and ^{13}C NMR spectra

3,6-Dibromo-2,7-di-*tert*-butyl-9,9-dimethyl-9*H*-thioxanthene 10,10-dioxide (3)

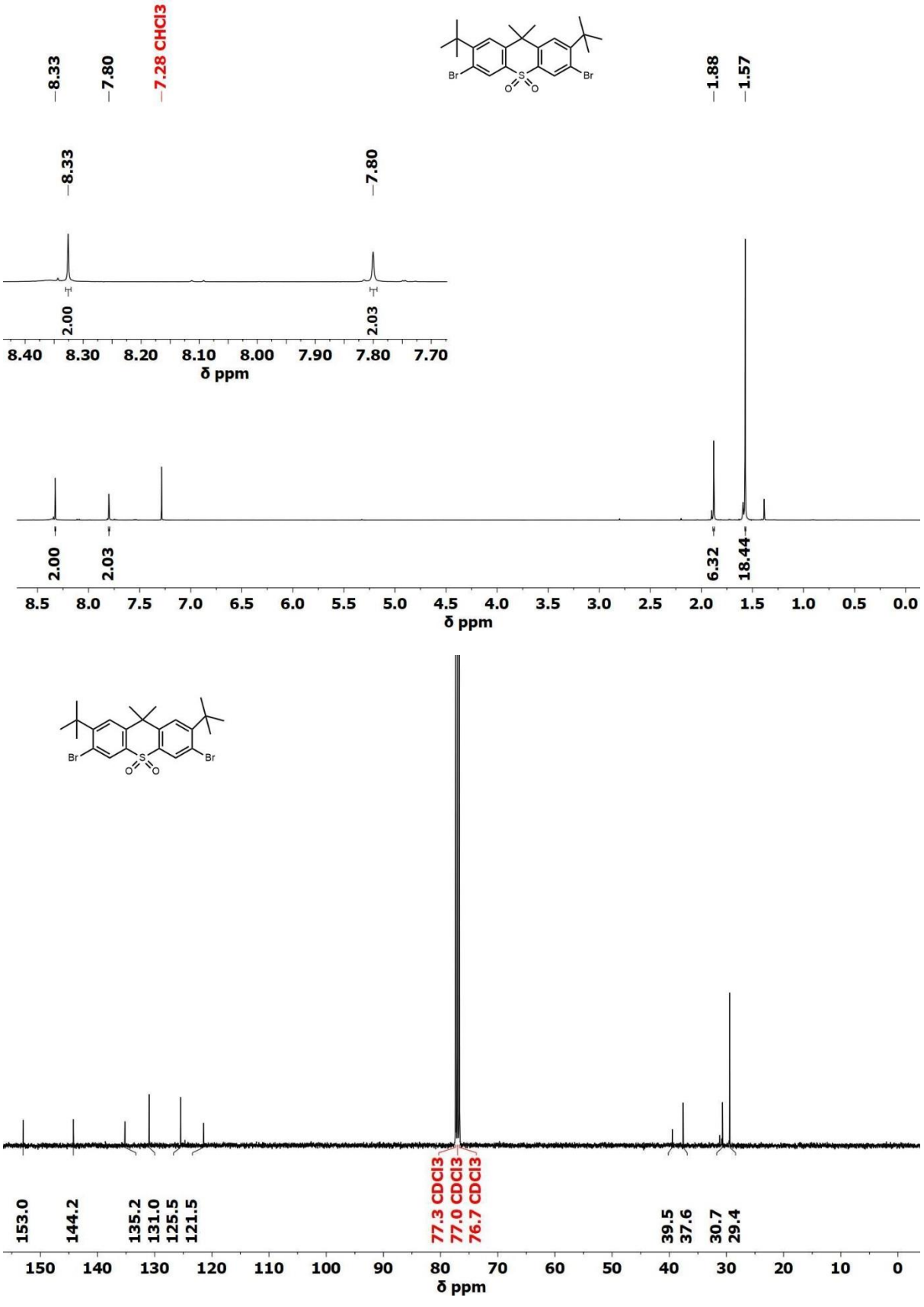

3,6-Dibromo-2,7-di-*tert*-butyl-9,9-dimethyl-9*H*-thioxanthene (4)

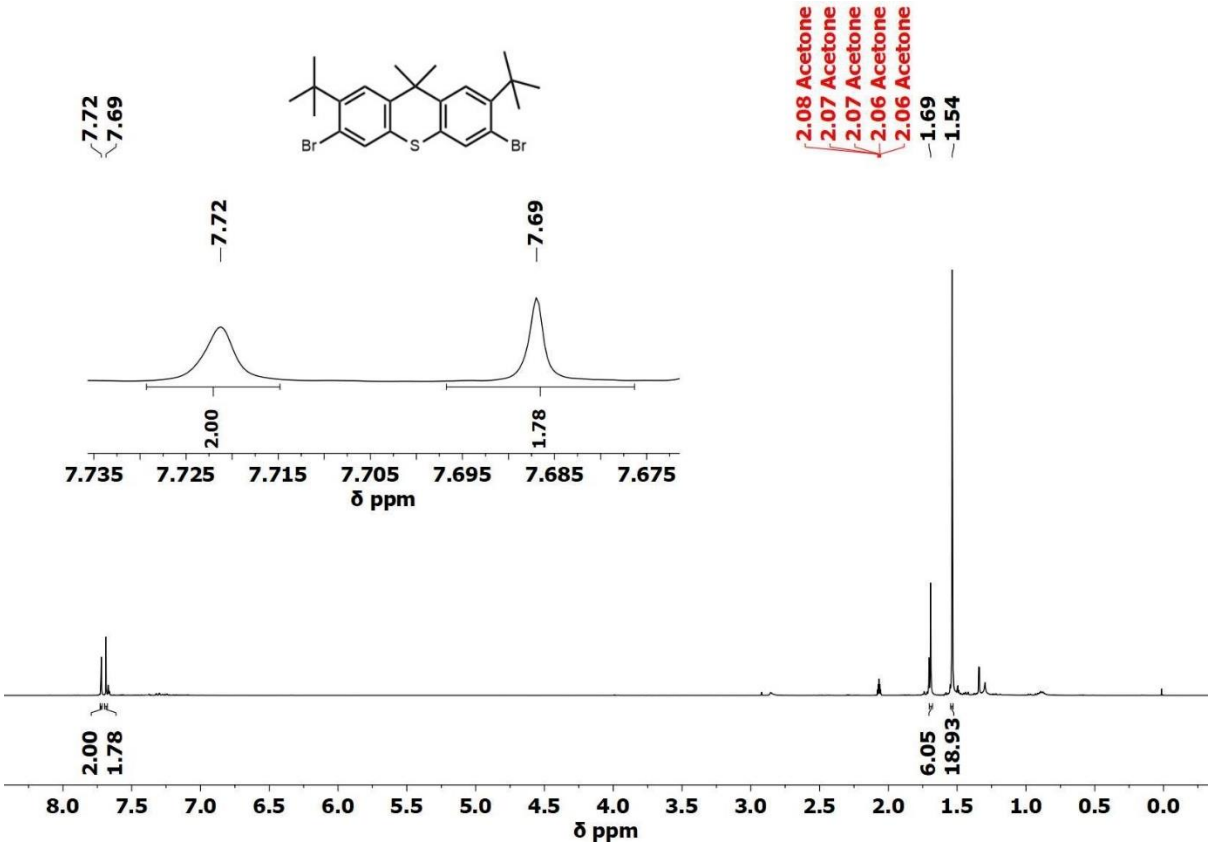

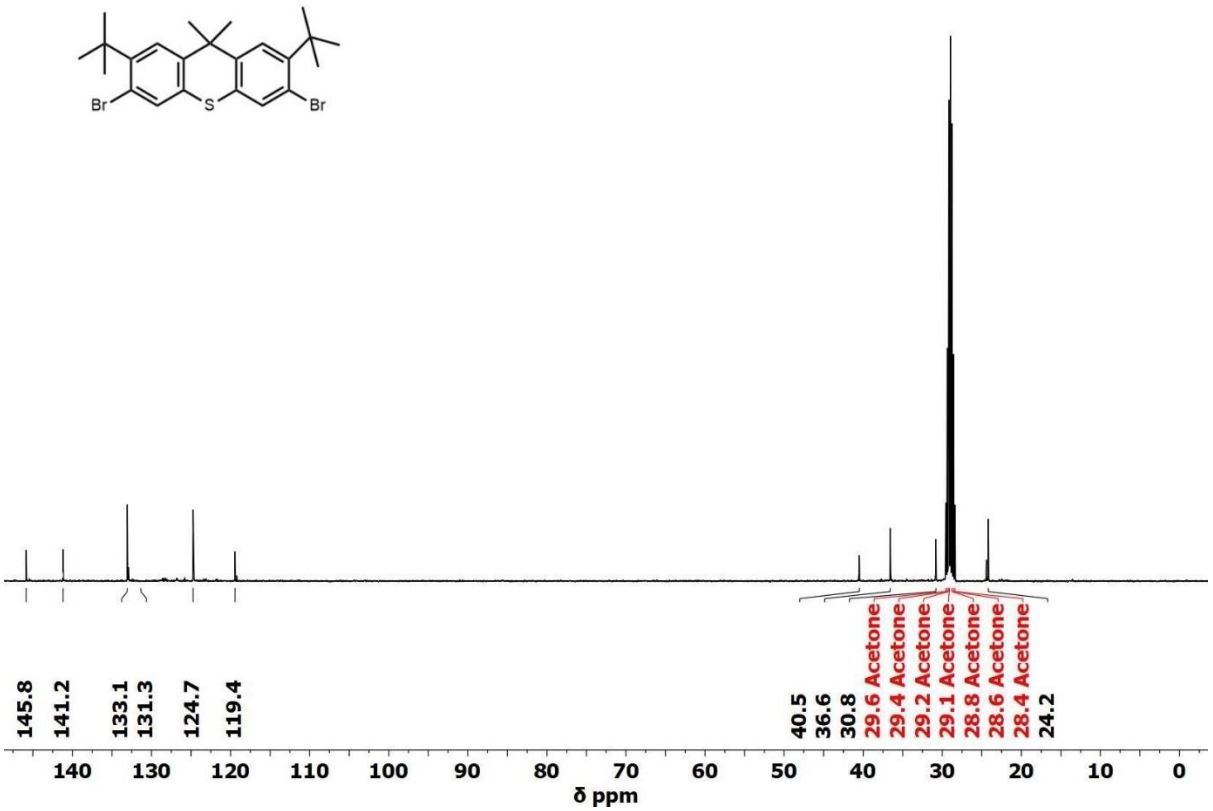

10,10'-(2,7-di-*tert*-butyl-9,9-dimethyl-9*H*-thioxanthene-3,6-diyl)bis(10*H*-phenothiazine) (*m*-^{t}BuTX-PTZ)

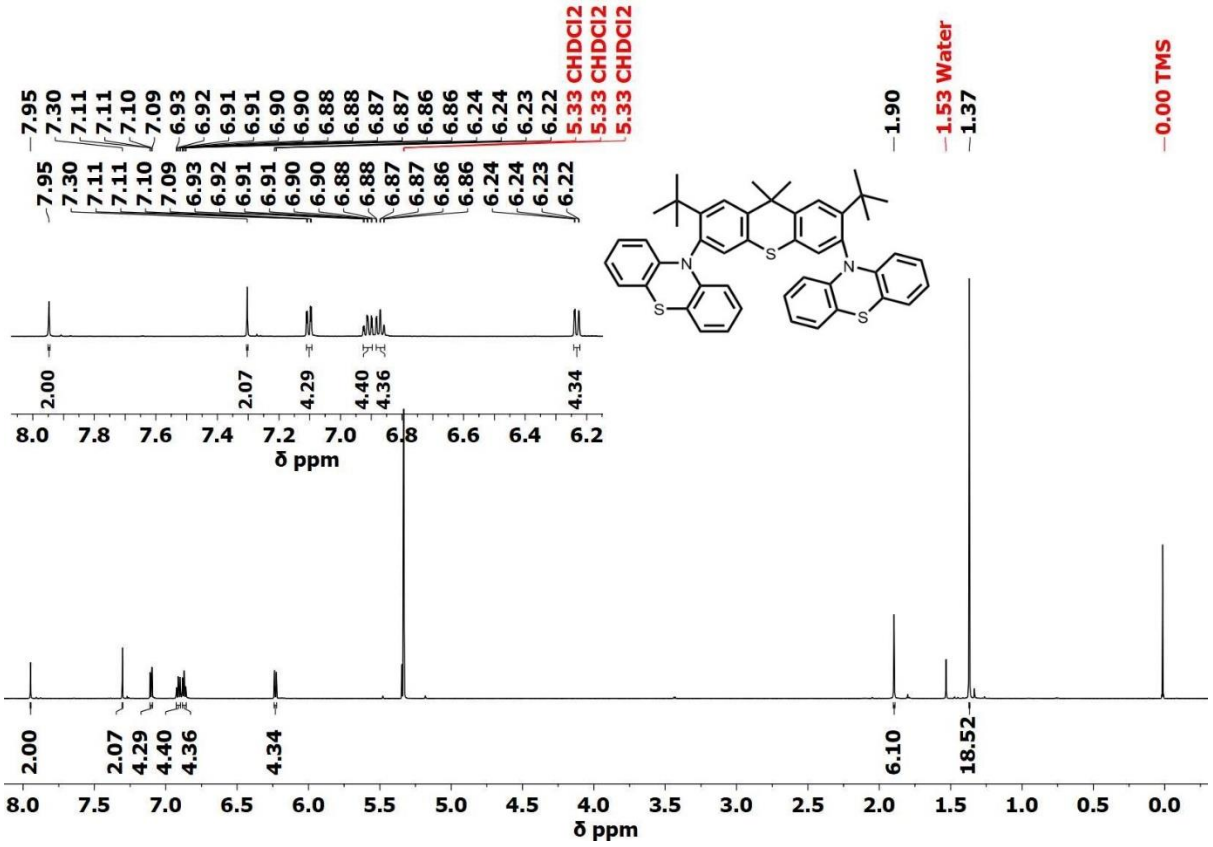

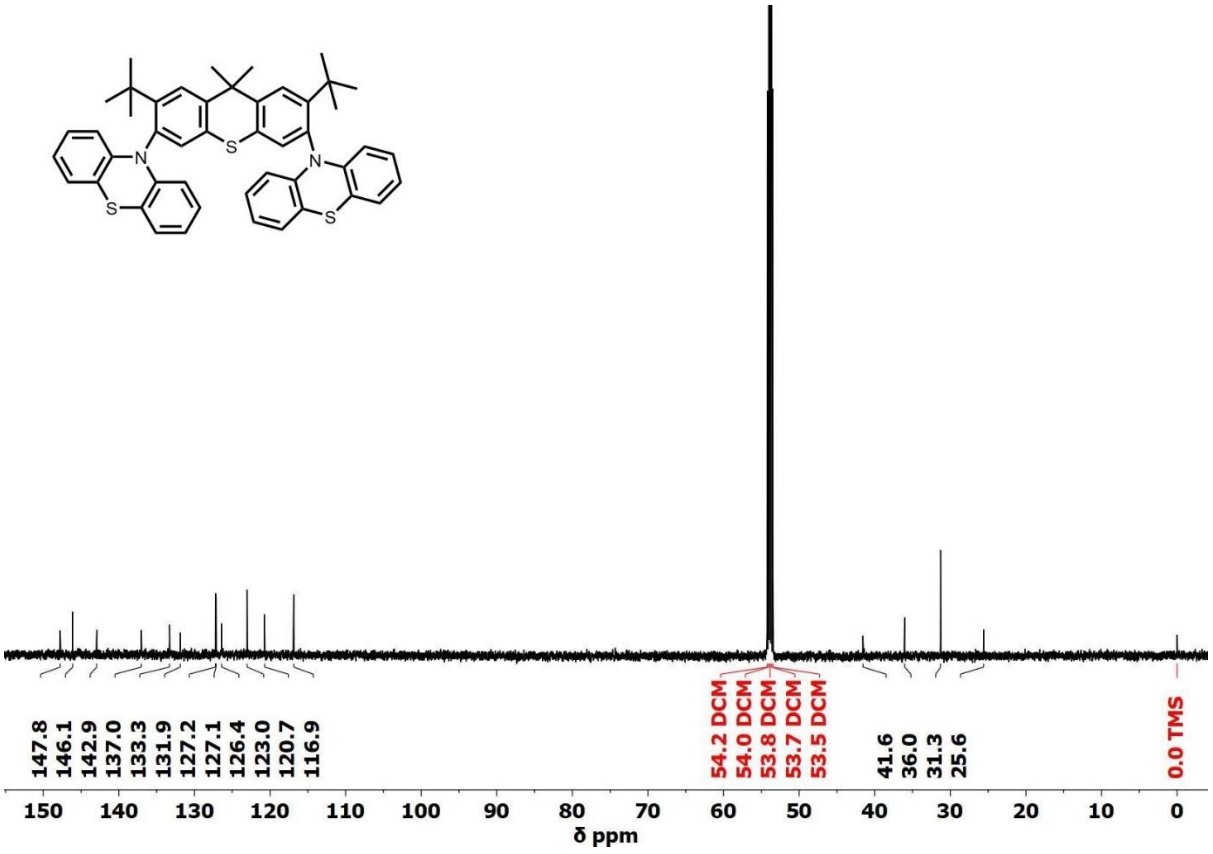

10,10'-(2,7-Di-*tert*-butyl-9,9-dimethyl-9*H*-thioxanthene-4,5-diyl)bis(10*H*-phenothiazine) (*o*-^{t}BuTX-PTZ)

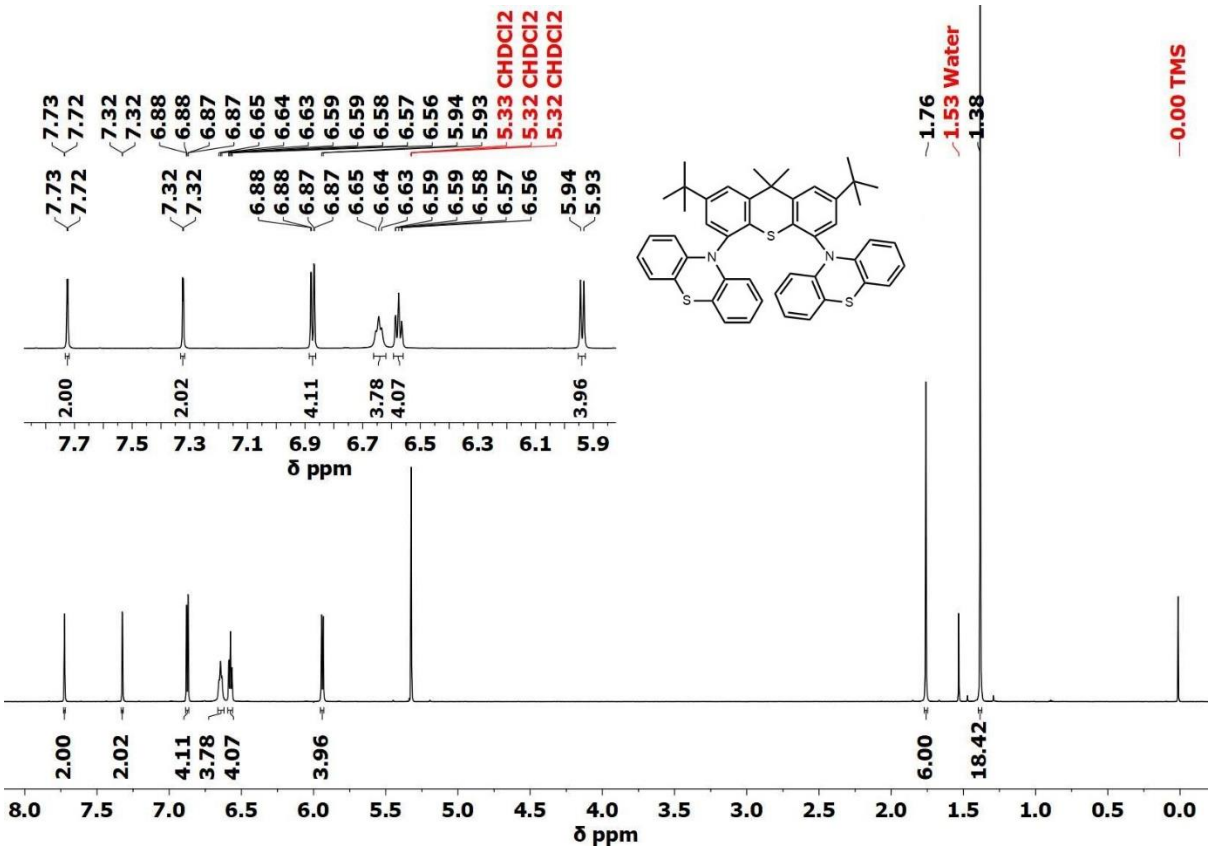

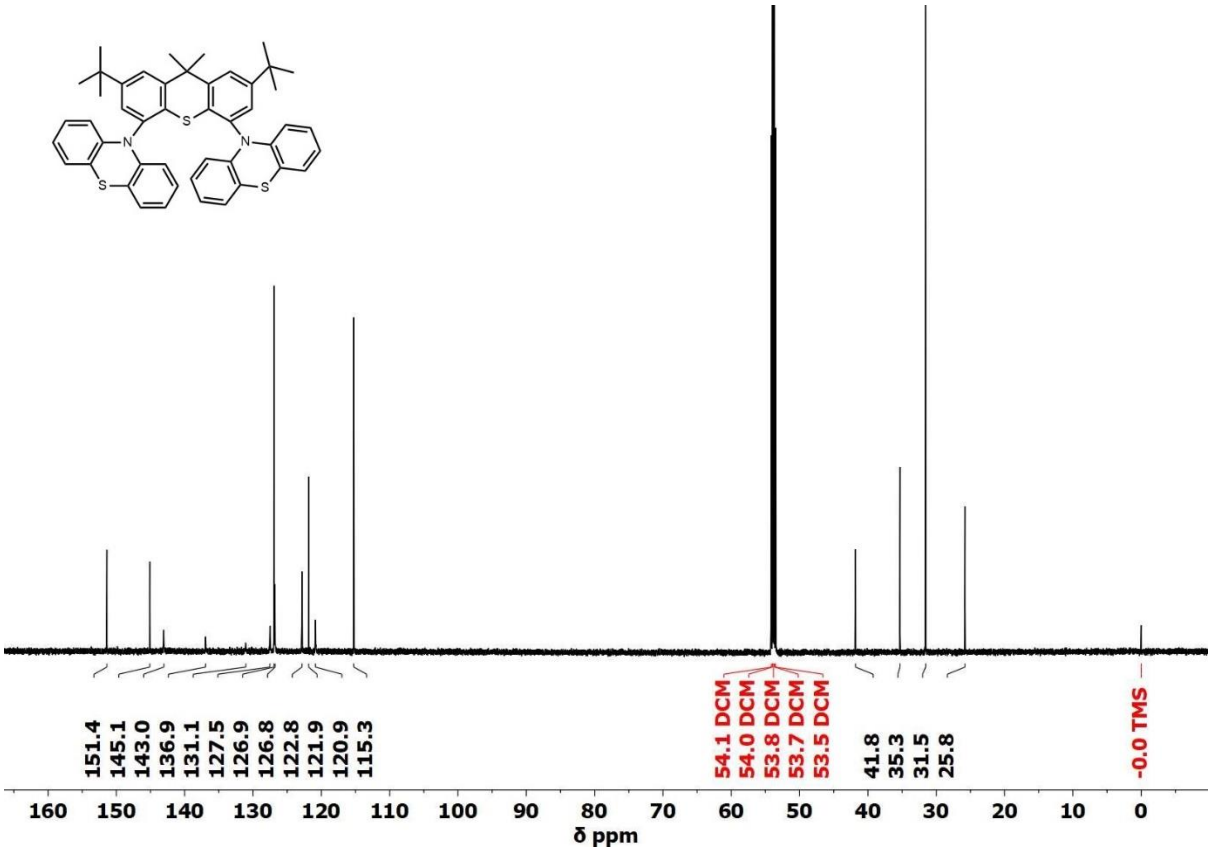

3,6-Dibromo-9,9-dimethyl-9*H*-thioxanthene (8)

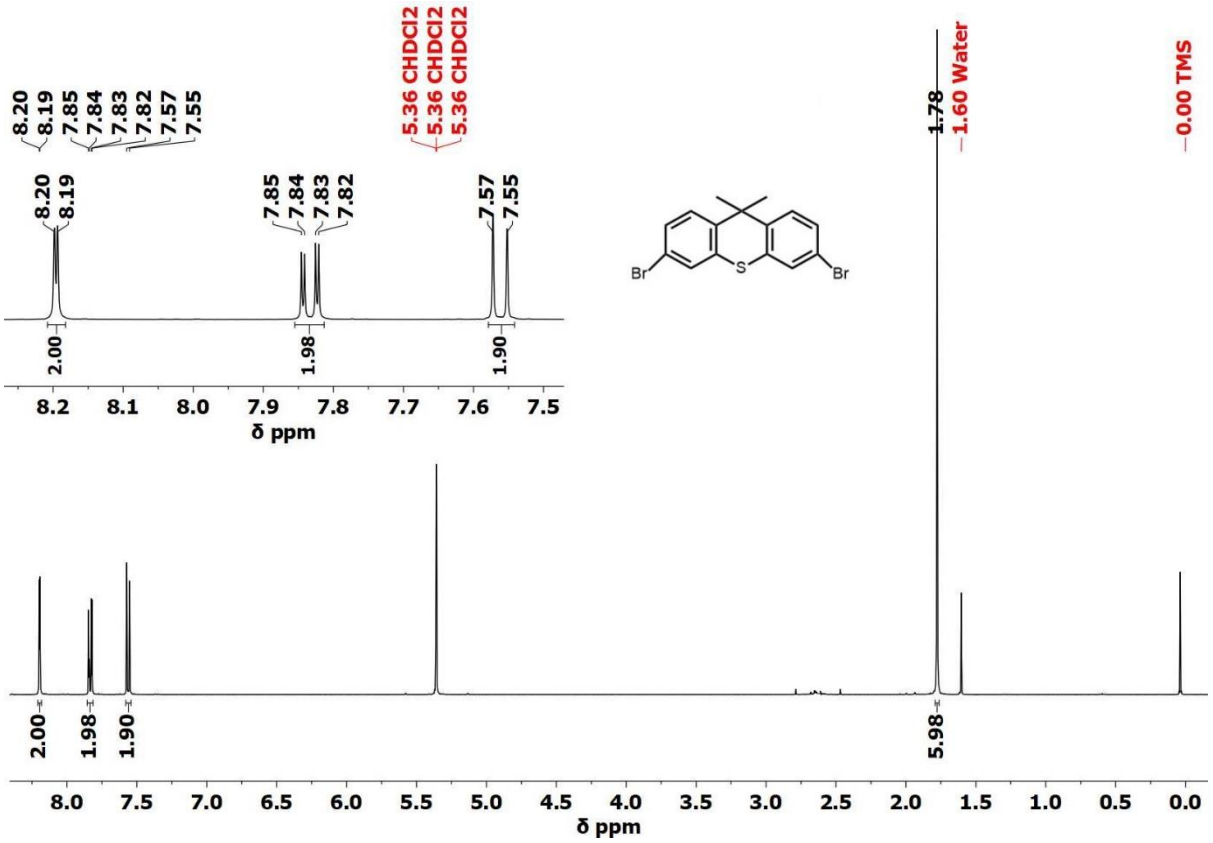

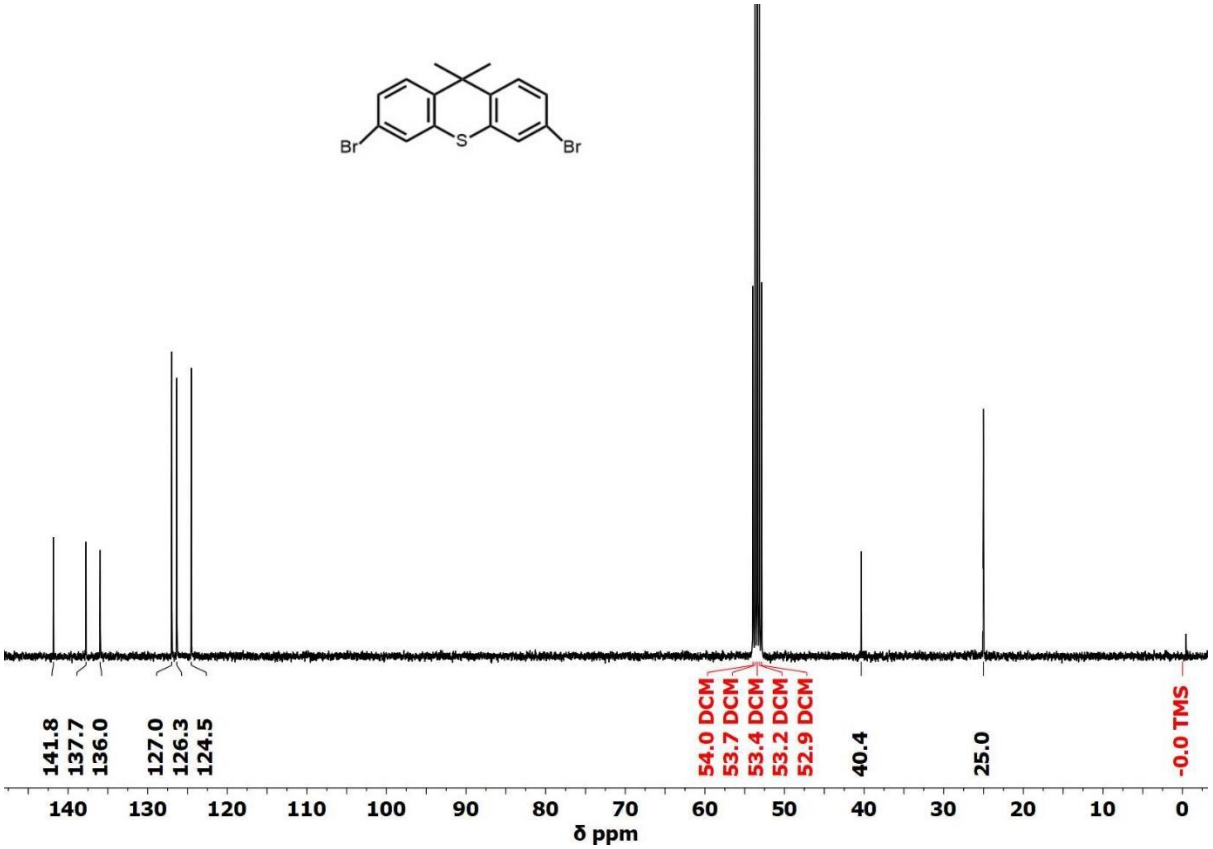

(3,6-Dibromo-9,9-dimethyl-9*H*-thioxanthene-2,7-diyl)bis(phenylmethanone) (9)

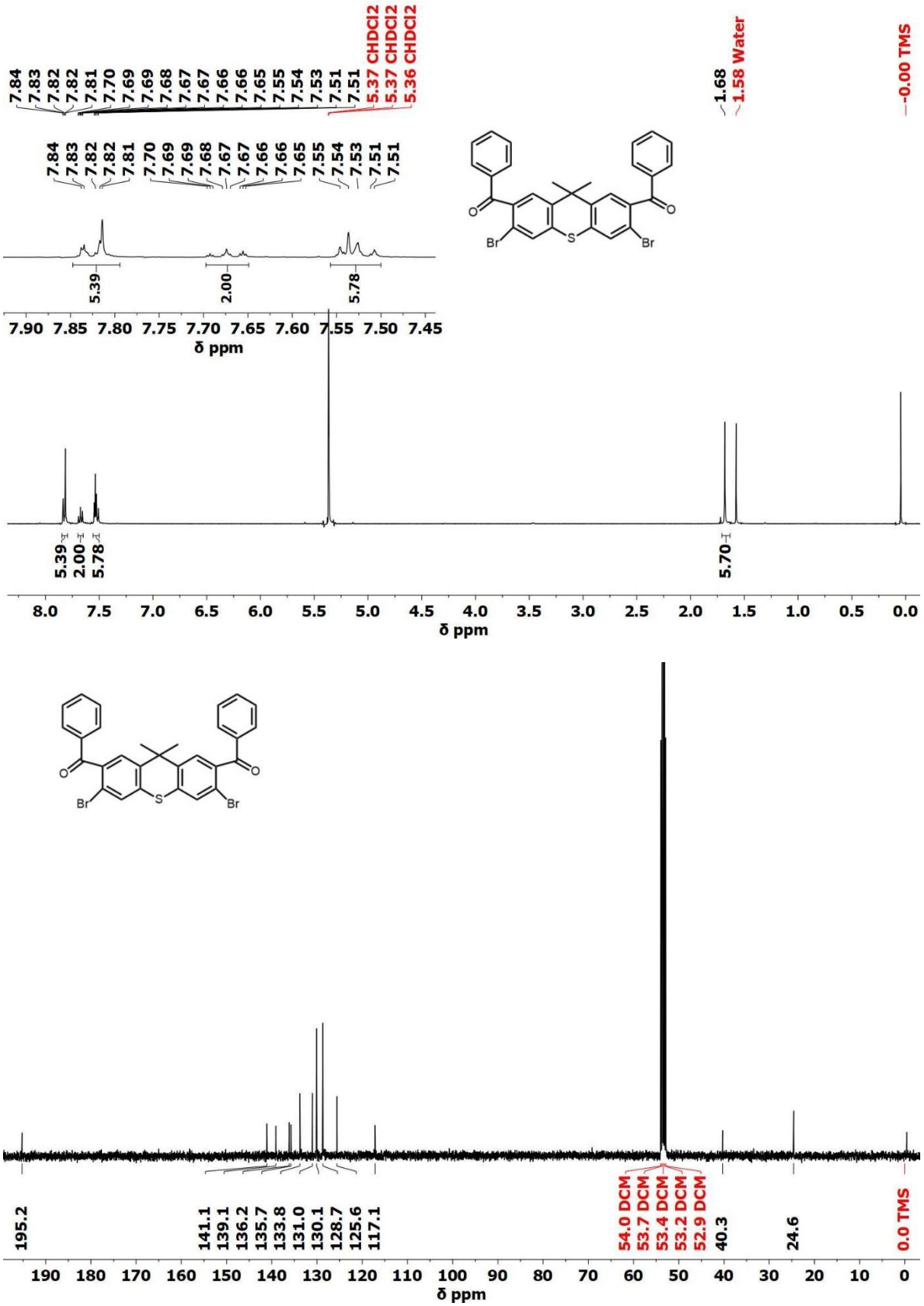

(9,9-Dimethyl-3,6-di(10*H*-phenothiazin-10-yl)-9*H*-thioxanthene-2,7-diyl)bis(phenyl-methanone) (*m*-BTX-PTZ)

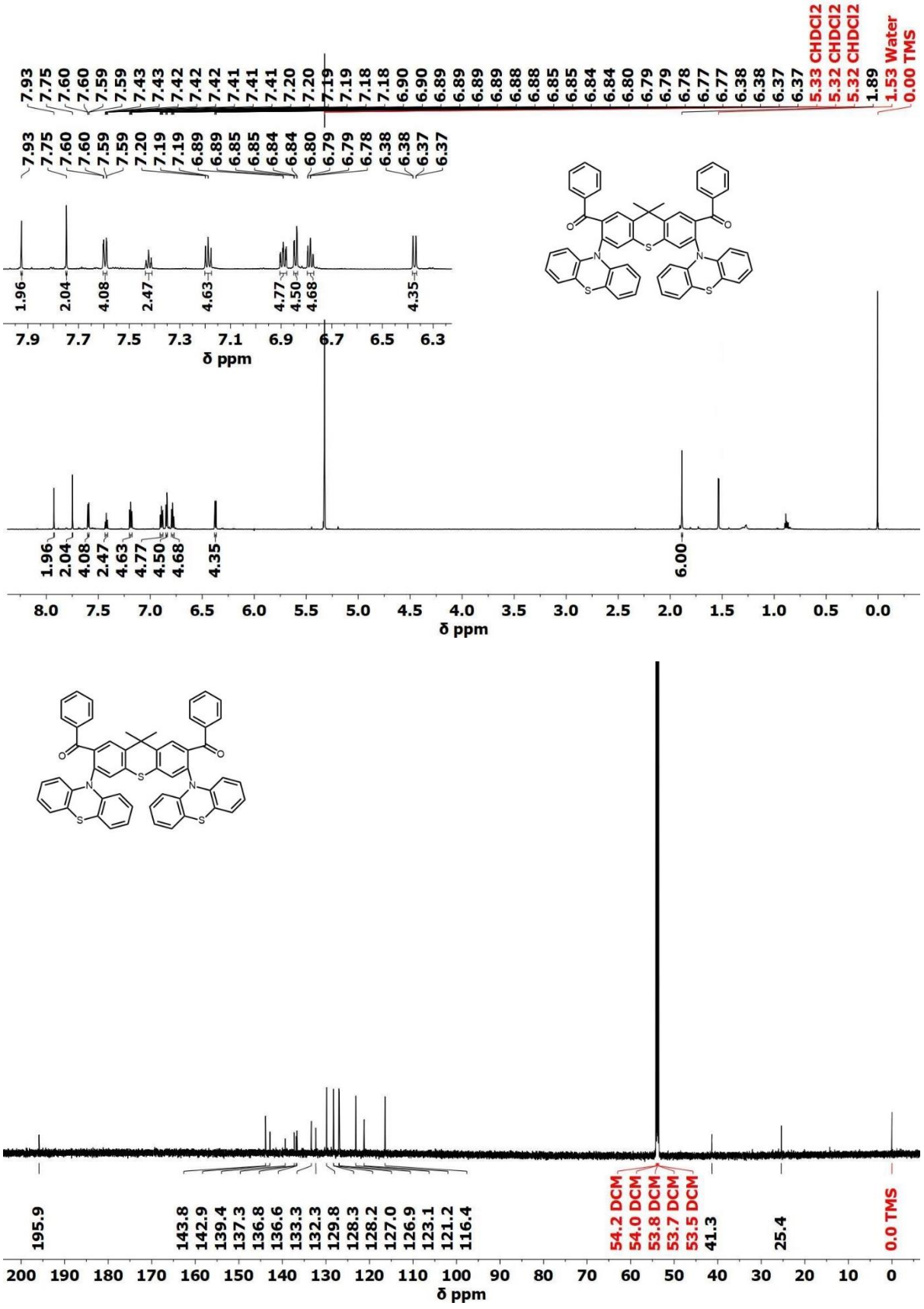

S2. Thermal properties

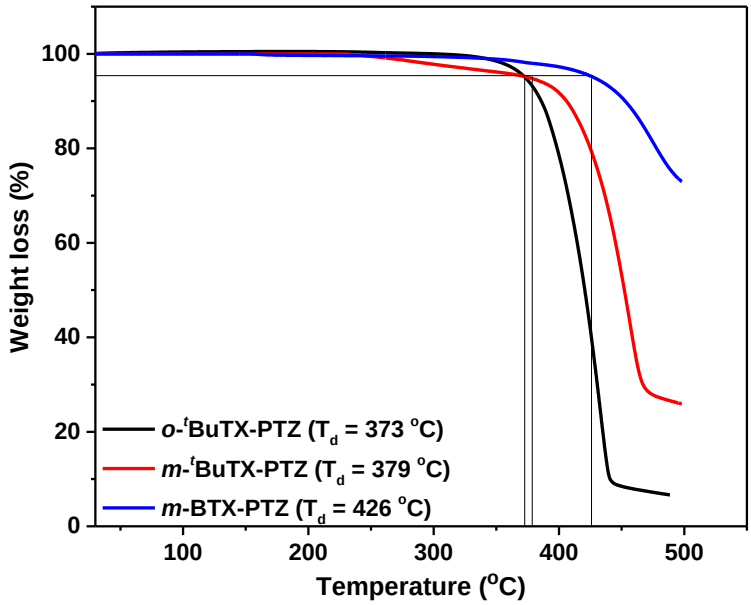

Figure S1. TGA analysis under N_2 with ramping temperature at 10 °C min^{-1} for compounds ***o*-^{t}BuTX-PTZ**, ***m*-^{t}BuTX-PTZ** and ***m*-BTX-PTZ** with reported 5% wt. loss values.

Thermal stability of the derivatives was probed by thermal gravimetric analysis (TGA). The TGA curves along with the decomposition temperatures (T_d) at the 5% wt. loss points are presented in **Figure S1**. The T_d values increase in the sequence ***o*-^{t}BuTX-PTZ** < ***m*-^{t}BuTX-PTZ** < ***m*-BTX-PTZ**. While the T_d values of *tert*-butyl substituted compounds are similar with ***m*-^{t}BuTX-PTZ** having by 6 °C higher decomposition temperature than ***o*-^{t}BuTX-PTZ**, introduction of bulkier benzoyl groups greatly improves thermal stability by increasing T_d by ca. 50 °C.

S3. X-ray crystallography

X-ray diffraction experiments for ***o*-^{t}BuTX-PTZ** and ***m*-^{t}BuTX-PTZ**·¼CH_2Cl_2 were carried out on a Bruker 3-circle D8 Venture diffractometer with a PHOTON 100 CMOS area detector, using Mo-*Kα* or Cu-*Kα* radiation from Incoatec IμS microsources with focussing mirrors. Crystals were cooled using a Cryostream (Oxford Cryosystems) open-flow N_2 gas cryostat. The data were processed using APEX3 v.2016.1-0 and reflection intensities integrated using SAINT v8.38A software (Bruker AXS, 2016). ***m*-^{t}BuTX-PTZ** was studied at Beamline I19 of Diamond Light Source (RAL) on a dual air-bearing fixed-χ diffractometer with pixel-array

photon-counting Dectris Pilatus 2M detector,[5] using undulator radiation monochromated with double-crystal Si(111). The crystal was cryo-mounted using remote-controlled BART robot[6] and cooled using a Cryostream N_2 gas cryostat. The diffraction images were converted to Bruker format using cbf_to_sfrm.py program[6] and further processed with APEX3 and SAINT software (*vide supra*).

m*-^{t}BuTX-PTZ·¼CH_2Cl_2** crystallized as 2-component non-merohedral twins related by a 180° rotation about the *z** axis (twin law -1 0 0 / 0 -1 0 / 0.526 0 1, the component ratio 0.625:0.375). The data were deconvoluted using CELL_NOW 2008/4 program and scaled using TWINABS 2012/1 program (G.M. Sheldrick, Bruker AXS). For the other compounds, the data were corrected for absorption by semi-empirical method based on Laue equivalents and multiple scans using SADABS 2016/2 program.[7] The structures were solved by direct methods using SHELXS 2013/1 software[8] (m*-^{t}BuTX-PTZ·¼CH_2Cl_2** by dual-space intrinsic phasing method using SHELXT 2018/2 program[9]), and refined by full-matrix least squares using SHELXL 2018/3 software[10] on OLEX2 platform.[11]

The asymmetric unit of ***m*-^{t}BuTX-PTZ·¼CH_2Cl_2** comprises two host molecules of similar conformations and a DCM molecule with 50% occupancy.

Table S1. Crystal data and experimental details

Compound	***o*-BuTXPTZ**	***m*-BuTXPTZ-dcm**	***m*-BuTXPTZ**
CCDC	1935514	1935515	1935516
Formula	$C_{47}H_{44}N_2S_3$	$C_{47}H_{44}N_2S_3{\cdot}¼\ CH_2Cl_2$	$C_{47}H_{44}N_2S_3$
$D_{calc.}$/ g cm^{-3}	1.257	1.288	1.273
μ/mm^{-1}	0.23	2.33	0.21
Formula Weight	733.02	754.25	733.02
T/K	120	120	100
Crystal System	triclinic	monoclinic	orthorhombic
Space Group	P-1 (no. 2)	$P2_1/c$ (no. 14)	$Pccn$ (no. 56)
a/Å	9.4919(6)	20.322(3)	20.2149(8)
b/Å	10.7313(7)	16.976(2)	22.3756(9)
c/Å	20.4159(13)	23.167(2)	16.9054(7)
α/°	90.284(3)	90	90
β/°	96.059(3)	103.246(6)	90
γ/°	110.388(3)	90	90
V/Å^3	1936.5(2)	7779.9(16)	7646.7(5)
Z	2	8	8
λ/Å	0.71073	1.54184	0.6889
Radiation type	Mo-K$_\alpha$	Cu-K$_\alpha$	synchrotron
$2\Theta_{max}$/°	55	120	58
Refls. total	36687	58898	124320
Refls. unique	8880	15027	11236
Refls with $I > 2\sigma(I)$	6504	8845	9108
R_{int}	0.052	0.148	0.087
Parameters/restraints	486, 0	981, 901	485, 0
Δρ /eÅ^{-3}	0.42, -0.37	0.76, -0.54	0.65, -0.51
Goodness of fit	1.029	1.061	1.079
R_1, wR_2 [$I > 2\sigma(I)$]	0.041, 0.090	0.098, 0.245	0.047, 0.121
R_1, wR_2 (all data)	0.069, 0.010	0.177, 0.280	0.058, 0.128

S4. Theoretical calculations

The optimized ground state structures, the HOMO/LUMO maps and the main computed parameters of the most stable conformers (*syn-syn*, *anti-anti* and *syn-anti*) are presented in **Figure S2** and **Table S2**. Interestingly, the conformers feature slightly different HOMO/LUMO wavefunction distributions and energies, with the lowest E_{HOMO} detected for the most stable conformer in the case of each compound (**Table S2**). Comparing the energy difference between the conformers of each type, it can be concluded that for ***o*-^{t}BuTX-PTZ** and ***m*-^{t}BuTX-PTZ** the folding of the PTZ units inwards/outwards is almost barrierless (0.006-0.081 eV). In turn, the PTZ folding barrier in ***m*-BTX-PTZ** is much higher (up to 0.3 eV, **Table S2**) due to the presence of bulkier benzoyl groups. These observations point to the potential superposition of *syn/anti* conformers in the solutions and solid films of these compounds. The conformers can undergo mutual transformation in the case of *tert*-butyl-substituted ***o*-^{t}BuTX-PTZ** and ***m*-^{t}BuTX-PTZ** due to a negligible barrier, whereas the conformers form

independently after the synthesis of ***m*-BTX-PTZ** (larger barrier). The effects of the *syn/anti* conformers on the photophysics of the presented molecules will be discussed in Section S6.

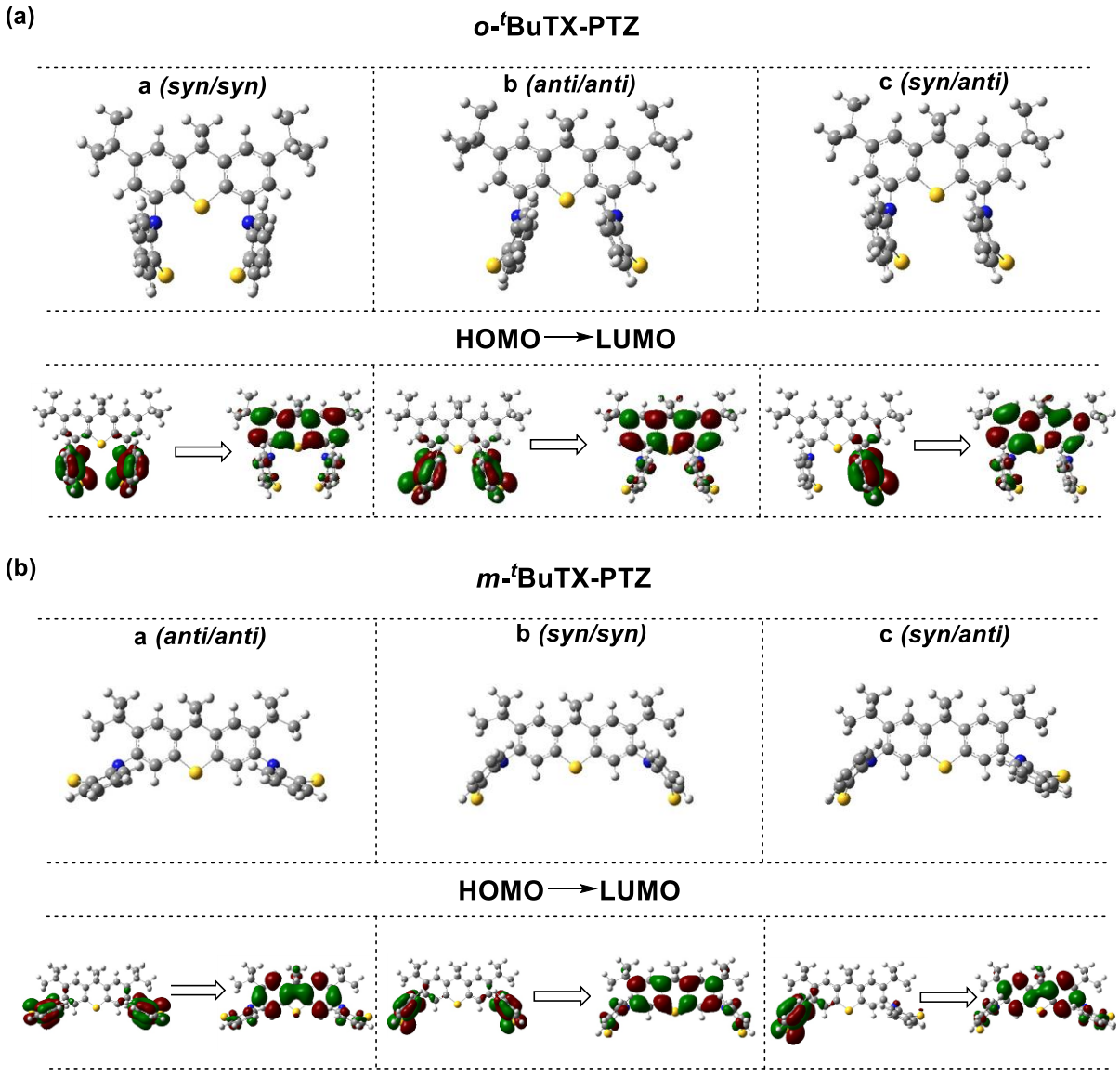

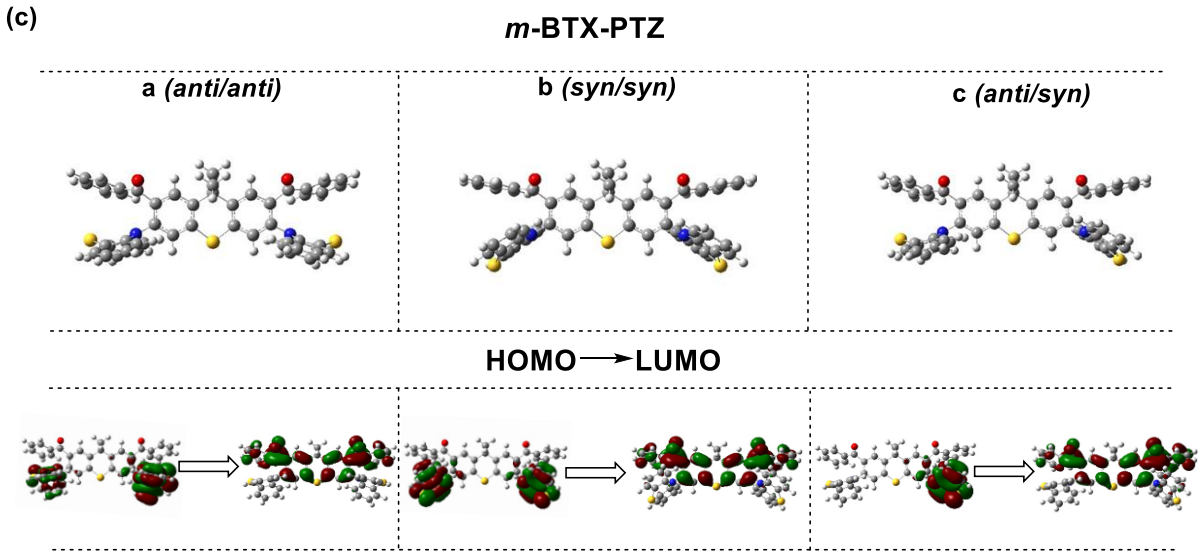

Figure S2. Ground state optimized geometries and HOMO/LUMO distributions of possible conformers of (a) ***o*-^{t}BuTX-PTZ,** (b) ***m*-^{t}BuTX-PTZ** and (c) ***m*-BTX-PTZ** (rBMK/6-31G(d)).

Table S2. Important calculated parameters of the possible conformers of ***m*-^{t}BuTX-PTZ**, ***o*-^{t}BuTX-PTZ** and ***m*-BTX-PTZ** (TDA-DFT rBMK/6-61G(d)).

	ΔE^a / [eV]	**E_{HOMO} / [eV]**	**E_{LUMO} / [eV]**	**S_1 / [eV]**	**$f_{S0\text{-}S1}$[b]**	**T_1 / [eV]**
***o*-^{t}BuTX-PTZ-(a)[c]**	0	-5.47	-0.06	3.95	0.0000	3.44
***o*-^{t}BuTX-PTZ-(b)**	0.031	-5.44	-0.06	3.88	0.0000	3.31
***o*-^{t}BuTX-PTZ-(c)**	0.006	-5.40	-0.03	3.89	0.0042	3.32
***m*-^{t}BuTX-PTZ-(a)**	0	-5.68	-0.18	3.87	0.0005	3.35
***m*-^{t}BuTX-PTZ-(b)**	0.081	-5.59	-0.13	3.79	0.0097	3.22
***m*-^{t}BuTX-PTZ-(c)**	0.042	-5.62	-0.12	3.79	0.0069	3.22
***m*-BTX-PTZ-(a)**	0	-5.86	-1.14	3.36	0.0131	3.18
***m*-BTX-PTZ-(b)**	0.296	-5.61	-1.21	3.09	0.0081	2.96
***m*-BTX-PTZ-(c)**	0.149	-5.62	-1.18	3.08	0.0067	2.97

[a]Energy difference between the conformers. [b]Oscillator strength. Zero stands for the minimum energy conformer. [c] **(a)**, **(b)** and **(c)** refer to the *syn/syn*, *anti/anti* and *syn/anti* conformers, respectively, identified in Figure S1.

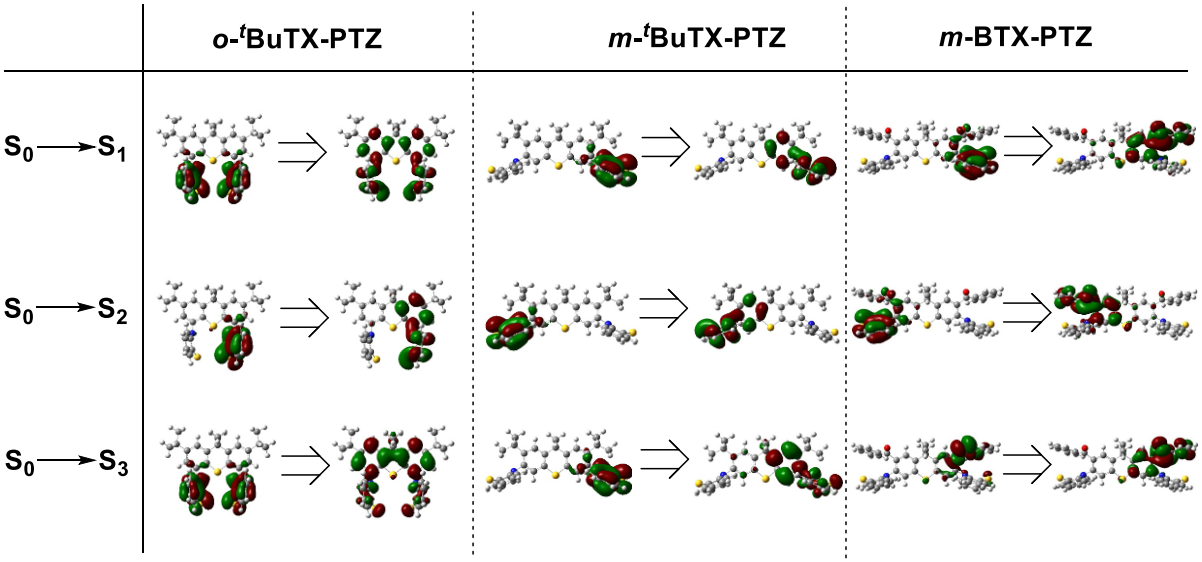

Figure S3. Selected set of singlet and triplet NTOs of the minimum energy conformers of ***m*-^{t}BuTX-PTZ**, ***o*-^{t}BuTX-PTZ** and ***m*-BTX-PTZ** (TDA-DFT rBMK/6-61G(d)).

The UV/Vis spectra were also calculated for the possible *syn/anti* conformers of the derivatives (**Figure S4**). Up to 7 nm red-shift, narrowing of the absorption spectra and a change in the S_0-S_1 transition oscillator strength (**Table S2**) were observed with the change of the conformation of the PTZ unit. Thus, it can be speculated that in the experimental spectra the average absorption of all the possible conformers is detected. Interestingly, the profile and position of absorption bands remain almost unchanged for ***m*-BTX-PTZ**, suggesting that introduction of the stronger acceptor and CT enhancement help to stabilize the optical characteristics. Evidently, different spectral profiles of the *syn/anti* conformers also imply a change in the NTO distribution.

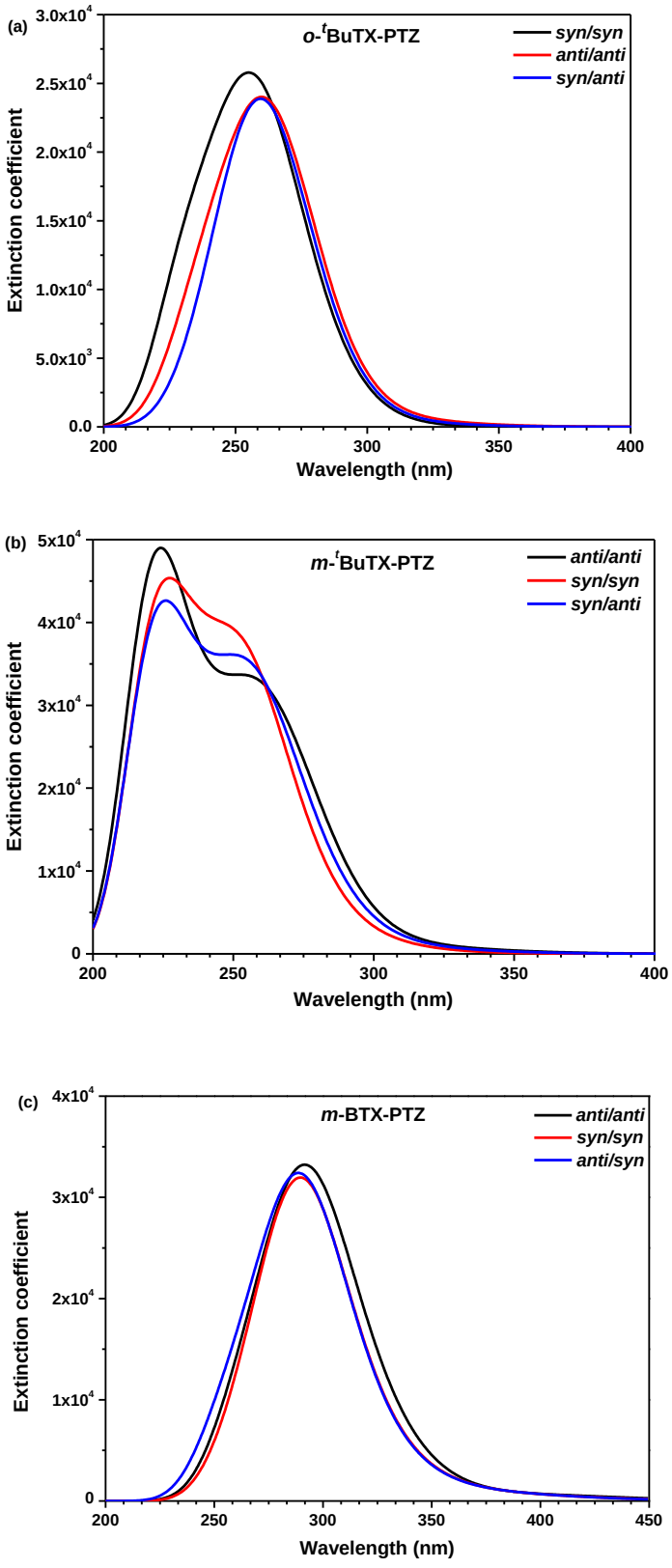

Figure S4. Theoretically predicted UV/Vis absorption spectra of possible conformers of (a) ***o*-^{t}BuTX-PTZ,** (b) ***m*-^{t}BuTX-PTZ** and (c) ***m*-BTX-PTZ** (TDA-DFT rBMK/6-31G(d)).

S5. Cyclic voltammetry measurements

Electrochemical measurements were performed in solutions of 0.1 M Bu_4NBF_4 (99%, Sigma Aldrich, dried) in dichloromethane (DCM, 99.9%, Extra Dry, stabilized, AcroSeal®, Acros Organics) at room temperature. Solutions were prepared with 1.0 mM concentrations of the D–A–D compounds and purged with nitrogen prior to measurement. The electrochemical cell comprised three electrodes: working (Pt disc 1 mm of diameter), counter (Pt wire), reference (Ag/AgCl). All cyclic voltammetry (CV) measurements were performed at room temperature with a potential scan rate of 50 mV/s and calibrated against a ferrocene/ferrocenium (Fc/Fc^+) redox couple.

The onset potential was determined from the intersection of two tangents drawn at the rising and background current of the CV. The ionization potential (IP) was calculated from the oxidation (E_{ox}) potential, using the following equation: $IP = E_{ox} + 5.1$.[14] HOMO energy levels were determined using CV analysis by the estimation of IPs which are similar to the HOMO energies.[15] As the reduction potentials were out of range even in DMF solution, LUMO energies were calculated according to the optical band gap E_g, which was determined from the onset of the UV-Vis absorption band in DCM.

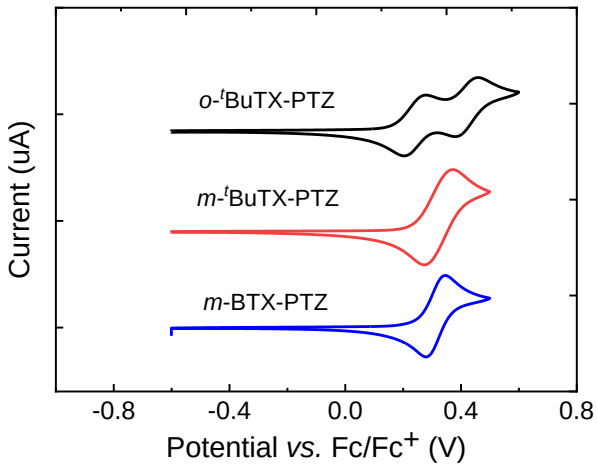

Figure S5. Cyclic voltammograms of the investigated molecules ***o*-^{t}BuTX-PTZ**, ***m*-^{t}BuTX-PTZ** and ***m*-BTX-PTZ** with 1 mM concentration in DCM solution.

Table S3. HOMO and LUMO energy levels and band gaps of ***o*-^{t}BuTX-PTZ**, ***m*-^{t}BuTX-PTZ** and ***m*-BTX-PTZ.**

Molecule	HOMO (eV)	LUMO (eV)	E_g (eV)
***o*-^{t}BuTX-PTZ**	-5.26	-1.89	3.37
***m*-^{t}BuTX-PTZ**	-5.34	-1.91	3.43
***m*-BTX-PTZ**	-5.35	-2.03	3.37

While only a single reversible oxidation peak is observed for the *meta*-substituted ***m*-^{t}BuTX-PTZ** and ***m*-BTX-PTZ**, interestingly, two reversible oxidation processes are detected for ***o*-^{t}BuTX-PTZ**. We tentatively attribute the appearance of the second peak to the additional through-space interaction of the phenothiazine donors induced by *ortho*-substitution.

S6. Photophysical characterization

Two types of samples were studied in this work: solutions (10^{-4} to 10^{-5} M) and films produced in zeonex (1% *w/w*) or DPEPO (10% *w/w*). All of the solutions were diluted in different solvents (ethanol, dichloromethane, toluene and methylcyclohexane) and stirred for up to 24 h. Films in matrix were fabricated by drop-casting onto sapphire substrates. Steady-state absorption and emission spectra were acquired using a UV-3600 Shimadzu spectrophotometer and a Jobin Yvon Horiba Fluoromax 3, respectively. PLQYs were recorded using a QE *Pro* Spectrophotometer (Ocean Optics) using 365 nm excitation.

Prompt fluorescence (PF), delayed fluorescence (DF) and phosphorescence spectra and time-resolved decays were recorded using nanosecond gated luminescence and lifetime measurements (from 800 ps to 1 s) with either a high energy pulsed Nd:YAG laser emitting at 355 nm (EKSPLA) or a N_2 laser emitting at 337 nm with pulse width of 170 ps. Emission was focused onto a spectrograph equipped with 300 lines/mm grating of 500 nm blaze wavelength and detected on a sensitive gated iCCD camera (Stanford Computer Optics) with sub-nanosecond resolution. Time-resolved measurements were performed by exponentially increasing the gate and delay times. The delay and integration times are chosen in a way that the next delay is set at a time longer than the previous delay+integration time. Therefore, no temporal overlap exists between the spectra corresponding to successive delays. The curve obtained directly from this process does not represent the real luminescence decay. However, this is easily corrected by integrating the measured spectra and dividing the integral by the corresponding integration time. In this way, each experimental point represents a snap-shot of the number of photons emitted per second at a time t = delay + (integration time)/2. The

luminescence decay is then obtained by plotting each experimental point versus time, and fitting with sum of exponentials when required. In this way the entire emission spectrum decaying over 8 decades is collected in a single experiment.[12] For initial development of these methods see previously published literature.[13]

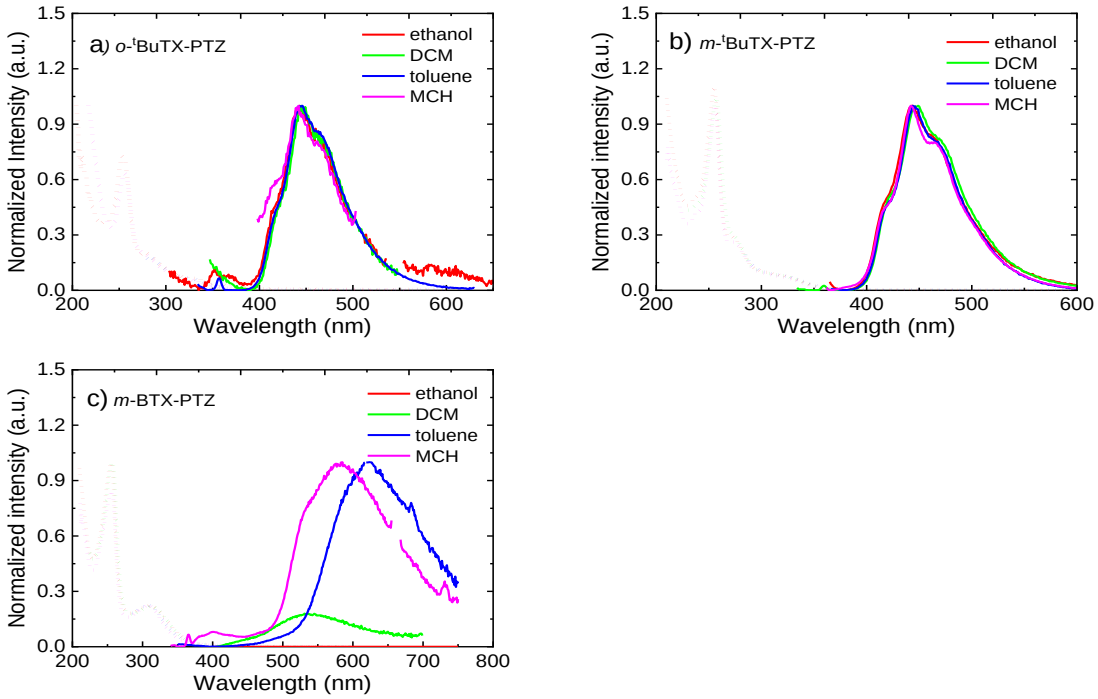

Figure S6. The normalized absorption and emission spectra in various solvents of a) ***o*-^{t}BuTX-PTZ**, b) ***m*-^{t}BuTX-PTZ** and c) ***m*-BTX-PTZ** at room temperature. The second harmonic (650 nm) in MCH is removed in c).

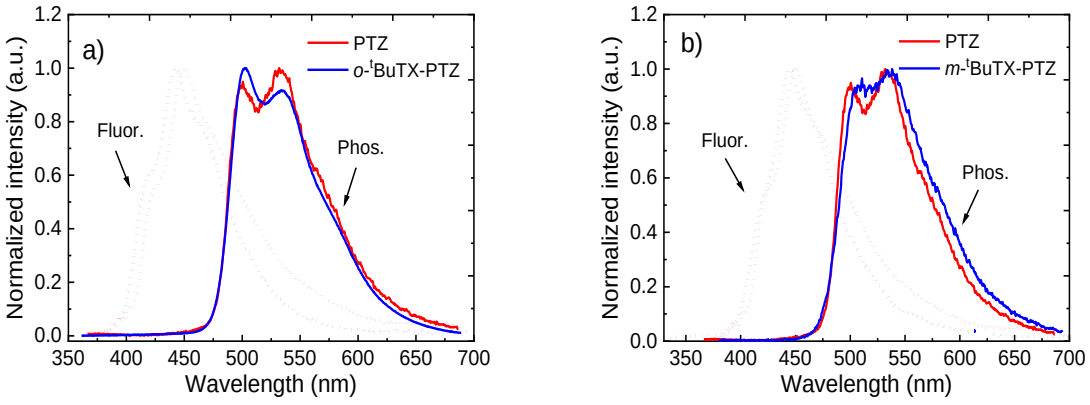

Figure S7. The comparison of fluorescence (dotted line) and phosphorescence (solid line) spectra of a) ***o*-^{t}BuTX-PTZ** and b) ***m*-^{t}BuTX-PTZ** in zeonex matrix (1 wt%) with the corresponding donor PTZ unit, all collected at 80 K.

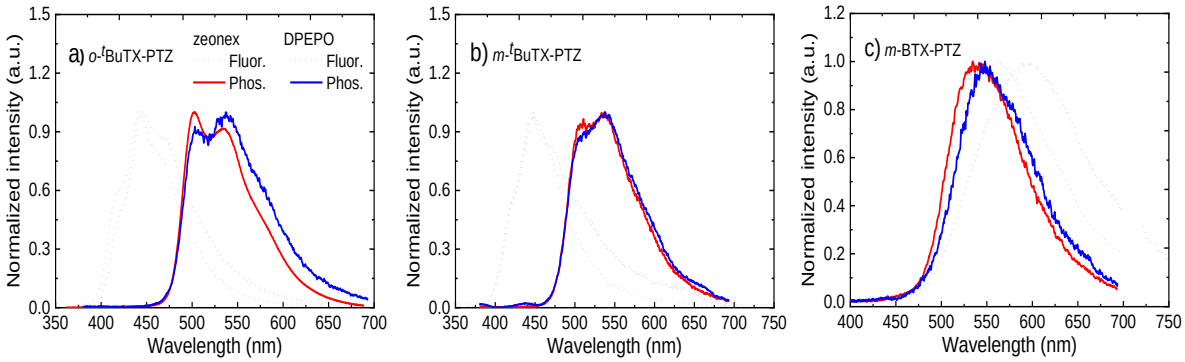

Figure S8. Fluorescence (dot) and phosphorescence (solid) spectra of a) ***o*-ᵗBuTX-PTZ**, b) ***m*-ᵗBuTX-PTZ** and c) ***m*-BTX-PTZ** in zeonex (1 wt%, red) and DPEPO (10 wt%, blue), all collected at 80 K.

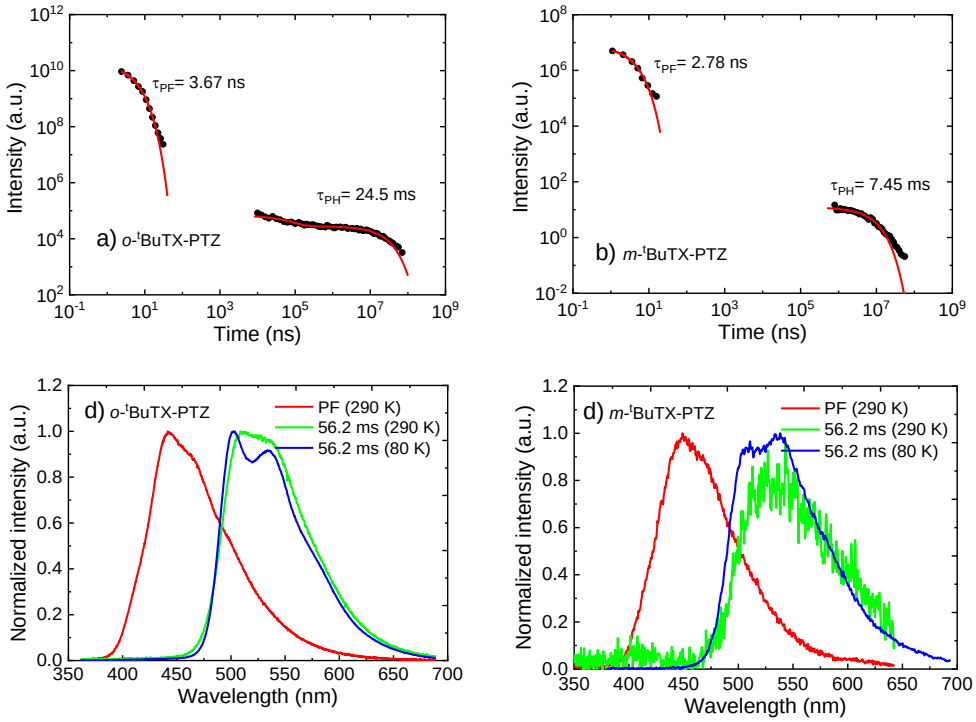

Figure S9. Time-resolved decays of a) ***o*-ᵗBuTX-PTZ** and b) ***m*-ᵗBuTX-PTZ** in zeonex matrix (1 wt%) at room temperature in oxygen-free condition. Time-resolved spectra of c) ***o*-ᵗBuTX-PTZ** and d) ***m*-ᵗBuTX-PTZ** in zeonex films, showing prompt fluorescence (red, 1.1 ns) collected at 290 K and phosphorescence (56.2 ms) recorded at 290 K (green) and 80 K (blue).

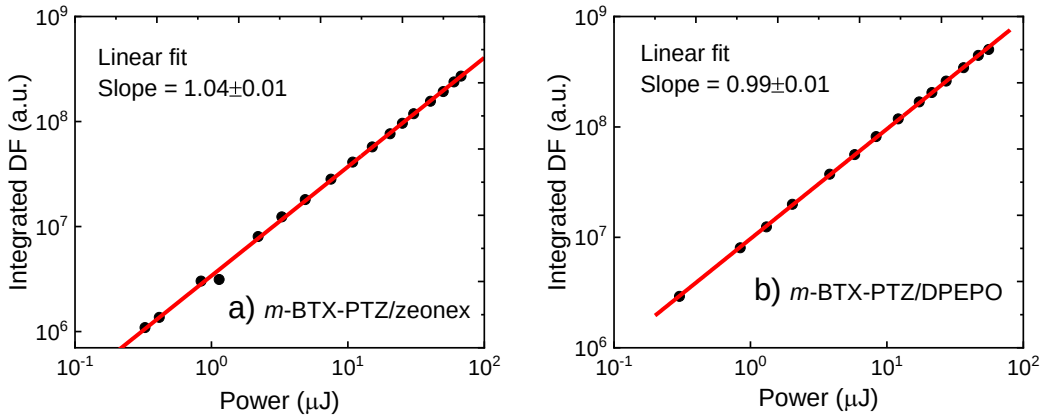

Figure S10. DF intensity as a function of laser influence of ***m*-BTX-PTZ** in a) zeonex matrix (1 wt%) and b) DPEPO (10 wt%), recorded at delay and integration times of 1 μs/1 ms and 0.5 μs/2 ms, respectively, at room temperature.

S7. Computational atomic coordinates

o-^{t}BuTX-PTZ

C	3.82144000	1.27713400	0.01738300
C	1.37993300	1.15556500	-0.01721200
C	1.30497200	2.55770400	-0.02180100
C	2.51981100	3.27846400	-0.00786500
C	3.78409200	2.68171800	0.01398100
C	-0.00007100	3.38307200	-0.06162300
C	-1.30507700	2.55766300	-0.02193100
C	-1.37999200	1.15552600	-0.01729300
C	-3.82150700	1.27704300	0.01715500
C	-3.78419100	2.68163100	0.01375100
C	-2.51992100	3.27840300	-0.00806400
H	4.76745300	0.73785600	0.03210900
H	2.46256100	4.36147900	-0.01559500
H	-4.76750700	0.73774000	0.03181800
H	-2.46268400	4.36142200	-0.01579500
C	5.09892800	3.48503700	0.03591500
C	5.94310300	3.12364600	-1.21380500
C	4.85484600	5.00988900	0.03149600
C	5.89743800	3.12366700	1.31553600
H	6.18295800	2.05310300	-1.24303100
H	5.40178500	3.37743200	-2.13505600
H	6.88962000	3.68183400	-1.20451000
H	4.28082600	5.33071500	0.91115800
H	5.81945100	5.53360100	0.05159200
H	4.31870600	5.33154600	-0.87141100
H	6.84123200	3.68578200	1.34283300
H	5.32083900	3.37233200	2.21652700
H	6.14052500	2.05401700	1.35066800

C	-5.09903800	3.48492600	0.03563700
C	-5.89755500	3.12356800	1.31526700
C	-4.85497200	5.00977800	0.03120900
C	-5.94319300	3.12350800	-1.21408200
H	-6.14061400	2.05391300	1.35042400
H	-5.32096500	3.37227300	2.21625400
H	-6.84136000	3.68566500	1.34254300
H	-4.31876200	5.33144000	-0.87165600
H	-5.81958700	5.53348400	0.05120000
H	-4.28105100	5.33063500	0.91092200
H	-6.88971600	3.68168400	-1.20479800
H	-5.40187000	3.37729100	-2.13533200
H	-6.18303700	2.05296200	-1.24330300
C	-0.00021900	4.34909300	1.16282200
H	-0.88430700	4.99615400	1.15552900
H	-0.00018800	3.77574600	2.09817300
H	0.88369900	4.99638400	1.15560300
C	-0.00003000	4.20866900	-1.38537200
H	0.00009900	3.53545200	-2.25171900
H	-0.88630200	4.85092500	-1.44924400
H	0.88613600	4.85108200	-1.44910100
S	-0.00001600	0.02095900	-0.03483000
C	2.93158100	-1.55675200	1.23872100
C	2.96133200	-1.55313600	-1.23484900
C	3.33322100	-0.84839000	2.38673100
C	2.75051900	-2.95199400	1.35246400
C	2.78233400	-2.94806400	-1.35683200
C	3.39098800	-0.84193500	-2.37103000
C	3.55465800	-1.51199400	3.59888300
H	3.46033600	0.22783900	2.33954400
C	3.01483600	-3.61352800	2.55591700
C	3.07508200	-3.60647500	-2.55539600
H	3.51831400	0.23396200	-2.31858000
C	3.64111700	-1.50251100	-3.57931300
C	3.40959800	-2.89754500	3.69083100
H	3.85291700	-0.93109600	4.46946600
H	2.88730000	-4.69371000	2.59756400
C	3.49733800	-2.88769000	-3.67856800
H	2.94816700	-4.68647400	-2.60289900
H	3.96117900	-0.91952300	-4.44070800
H	3.59461700	-3.41794600	4.62792100
H	3.70491100	-3.40545400	-4.61238500
C	-2.96098200	-1.55320600	-1.23505200
C	-2.93178200	-1.55681400	1.23853900
C	-3.39024600	-0.84196800	-2.37135200
C	-2.78201500	-2.94814000	-1.35699600
C	-2.75083600	-2.95206300	1.35231600
C	-3.33350500	-0.84843600	2.38652300
C	-3.64002700	-1.50250100	-3.57973400
H	-3.51754200	0.23393400	-2.31889600

C	-3.07441900	-3.60650600	-2.55566700
C	-3.01535900	-3.61358700	2.55573500
H	-3.46052900	0.22780400	2.33934500
C	-3.55514900	-1.51202400	3.59863900
C	-3.49628900	-2.88768100	-3.67896600
H	-3.95978800	-0.91947600	-4.44121500
H	-2.94755100	-4.68651100	-2.60316000
C	-3.41021800	-2.89759500	3.69060300
H	-2.88791100	-4.69378000	2.59737800
H	-3.85347200	-0.93110700	4.46918700
H	-3.70358400	-3.40543000	-4.61285400
H	-3.59540600	-3.41798800	4.62766500
C	2.64823800	0.52818900	0.00105000
C	-2.64828800	0.52812500	0.00091400
N	-2.70008700	-0.90319400	-0.00011100
N	2.70003500	-0.90313400	0.00002600
S	-2.05743800	-3.88130700	-0.01179600
S	2.05728500	-3.88112800	-0.01180400

_m_-^{t}BuTX-PTZ

C	-3.84419500	0.20419300	-0.02670100
C	-1.39229500	0.09559700	0.03149900
C	-1.30499700	1.49249700	-0.09700100
C	-2.52389800	2.18449500	-0.18350100
C	-3.81089700	1.61039300	-0.15650100
C	0.00030200	2.31969900	-0.13800100
C	1.30600300	1.49380100	-0.08960100
C	1.39370500	0.09670100	0.03659900
C	3.84560500	0.20650500	-0.01510100
C	3.81200300	1.61340400	-0.13880100
C	2.52480200	2.18680300	-0.17020100
H	-2.47180000	3.26459500	-0.27460100
H	2.47180000	3.26700300	-0.26090100
C	0.00360100	3.14929900	-1.45840100
H	0.88630000	3.79620000	-1.51550100
H	0.00950200	2.48099900	-2.32840100
H	-0.88330000	3.78959800	-1.52260100
C	-0.00420000	3.28329900	1.08839900
H	-0.00719900	2.71019900	2.02379900
H	0.88149900	3.92960000	1.08399900
H	-0.89010100	3.92919800	1.07789900
S	0.00090700	-1.01140100	0.18699900
C	-5.52969300	-0.93770900	1.31239900
C	-5.49999300	-1.19640900	-1.14840100
C	-4.73679400	-0.77500800	2.46649900
C	-6.82349300	-1.48221100	1.47819900
C	-6.79209200	-1.76501100	-1.22900100
C	-4.67849300	-1.27680800	-2.29120100

C	-5.21059300	-1.15620900	3.72669900
H	-3.74489400	-0.34460600	2.38149900
C	-7.27349200	-1.89811200	2.73519900
C	-7.21269100	-2.43231100	-2.38360100
H	-3.68639400	-0.83950600	-2.27480100
C	-5.12309200	-1.91100800	-3.45660100
C	-6.47479200	-1.73071000	3.87089900
H	-4.57119300	-1.00820800	4.59469900
H	-8.26779100	-2.33381300	2.81569900
C	-6.38609100	-2.50321000	-3.50950100
H	-8.20629100	-2.87691300	-2.39710100
H	-4.46229200	-1.94600700	-4.32050100
H	-6.83989200	-2.03981100	4.84759900
H	-6.72959000	-3.00861100	-4.40920100
C	5.50250700	-1.17799300	-1.15150100
C	5.52900700	-0.95289300	1.31299900
C	4.68220700	-1.23899400	-2.29630100
C	6.79260800	-1.74949100	-1.23850100
C	6.82050700	-1.50459100	1.47269900
C	4.73610600	-0.80139400	2.46859900
C	5.12630800	-1.85679400	-3.47050100
H	3.69130600	-0.79889600	-2.27300100
C	7.21280900	-2.40099100	-2.40240100
C	7.26760800	-1.93879100	2.72459900
H	3.74650600	-0.36499600	2.38799900
C	5.20720700	-1.20069300	3.72419900
C	6.38760900	-2.45209200	-3.53050100
H	4.46660800	-1.87689500	-4.33570100
H	8.20480900	-2.84898900	-2.42100100
C	6.46870800	-1.78279200	3.86179900
H	8.25980900	-2.38008900	2.80019900
H	4.56800700	-1.06069400	4.59359900
H	6.73060900	-2.94509100	-4.43720100
H	6.83160800	-2.10629100	4.83459900
C	-2.64769400	-0.52120500	0.06249900
C	2.64930600	-0.51969700	0.06819900
N	5.06120600	-0.55469400	0.03909900
N	-5.05989400	-0.55670800	0.03399900
S	7.97060700	-1.54218900	0.09769900
S	-7.97159300	-1.53331300	0.10189900
C	5.01070100	2.59430600	-0.23920100
C	4.93770000	3.58710600	0.95379900
C	6.41660200	1.95130800	-0.20970100
C	4.90140000	3.37960600	-1.57580100
H	4.00279900	4.16130500	0.96239900
H	5.01710100	3.04760600	1.90699900
H	5.77109900	4.30010700	0.89219900
H	6.57680300	1.26770800	-1.05050100
H	7.15780100	2.75860900	-0.28770100
H	6.60860300	1.41000900	0.72279900

H	5.73809900	4.08680700	-1.65670100
H	4.95030100	2.69220600	-2.43070100
H	3.96909900	3.95290500	-1.65170100
C	-5.01009900	2.59009200	-0.26270100
C	-4.88810000	3.38729200	-1.59120100
C	-6.41479800	1.94369000	-0.25450100
C	-4.95220000	3.57289200	0.93929900
H	-3.95680100	3.96369300	-1.65210100
H	-4.92599900	2.70719200	-2.45250100
H	-5.72570100	4.09299100	-1.67470100
H	-6.61889700	1.40238900	0.67529900
H	-7.15689900	2.74898900	-0.34340100
H	-6.56049700	1.25928900	-1.09750100
H	-5.78830100	4.28279100	0.87639900
H	-5.03769900	3.02459200	1.88679900
H	-4.01990100	4.15119300	0.96119900
H	2.71750700	-1.60309700	0.16219900
H	-2.71549300	-1.60410500	0.16209900

***m*-BTX-PTZ**

C	-3.83347600	-0.10353100	-0.20753500
C	-1.39165000	-0.17437900	-0.08519400
C	-1.30142600	1.22890800	-0.08970700
C	-2.51990000	1.92373000	-0.18936400
C	-3.77893400	1.30904200	-0.21723600
C	-0.00001700	2.05688900	-0.00016000
C	1.30139000	1.22887700	0.08921900
C	1.39161100	-0.17441300	0.08433700
H	-2.51423500	3.00884000	-0.24892400
C	0.09722000	2.95438800	-1.27153100
H	0.97724000	3.60591900	-1.22096500
H	0.17788200	2.33350100	-2.17233900
H	-0.78582900	3.59494000	-1.37384500
C	-0.09723300	2.95411400	1.27141100
H	-0.17796500	2.33303700	2.17208200
H	0.78586000	3.59458200	1.37389600
H	-0.97720800	3.60571100	1.22095300
S	-0.00002300	-1.28607500	-0.00054700
C	-5.83583800	-0.82642000	-1.42509200
C	-5.44755900	-1.49115700	0.96032800
C	-5.49156100	0.00882400	-2.50832500
C	-6.97929500	-1.64313400	-1.58307600
C	-6.53694900	-2.38743000	1.02177400
C	-4.76124300	-1.23373200	2.16699800
C	-6.28373400	0.07651300	-3.65985100
H	-4.59164700	0.61054300	-2.47621900
C	-7.78427400	-1.54311800	-2.72245000
C	-6.94308600	-2.94511400	2.23979800
H	-3.90526800	-0.56815800	2.16854000

C	-5.14894900	-1.82426100	3.37341300
C	-7.44861600	-0.68122900	-3.77002800
H	-5.97399500	0.73730100	-4.46673300
H	-8.66949700	-2.17335400	-2.78985300
C	-6.25229600	-2.67703600	3.42418800
H	-7.80265200	-3.61338800	2.24298100
H	-4.57840600	-1.60228100	4.27301100
H	-8.07783500	-0.62050900	-4.65473600
H	-6.56824800	-3.13257100	4.35968000
C	-2.63754500	-0.81936200	-0.16566700
N	-5.05225300	-0.85662600	-0.24391600
S	-7.37036600	-2.97238900	-0.44824200
H	-2.68561000	-1.90696600	-0.18091900
C	-4.96419300	2.23765400	-0.44418600
C	-6.23061600	2.09580100	0.34312900
O	-4.84479300	3.11883300	-1.27274000
C	-6.22581800	1.63341000	1.66603800
C	-7.43285600	2.52989500	-0.24356400
C	-7.41630700	1.58947700	2.39887600
H	-5.29282400	1.32145900	2.12663300
C	-8.62235200	2.46992400	0.48275000
H	-7.41234200	2.89988100	-1.26590400
C	-8.61452700	2.00092500	1.80515800
H	-7.40575100	1.23011400	3.42558000
H	-9.55598600	2.78820800	0.02297200
H	-9.54343200	1.95775400	2.37124700
C	2.51985400	1.92368100	0.18919200
C	3.77888800	1.30898800	0.21708800
H	2.51416400	3.00877500	0.24908900
C	3.83343000	-0.10357700	0.20704400
C	4.96408400	2.23756300	0.44457200
C	2.63750400	-0.81940700	0.16478300
N	5.05220000	-0.85667700	0.24352300
C	6.23074500	2.09592000	-0.34239300
O	4.84440800	3.11857300	1.27326700
H	2.68559200	-1.90702200	0.17978700
C	5.83547500	-0.82676300	1.42491800
C	5.44781300	-1.49094600	-0.96074900
C	6.22639200	1.63359500	-1.66532500
C	7.43275400	2.53017800	0.24465900
C	5.49091300	0.00824800	2.50823300
C	6.97885000	-1.64355800	1.58305400
C	6.53722500	-2.38721000	-1.02210600
C	4.76177900	-1.23329500	-2.16753200
C	7.41708900	1.58989900	-2.39783600
H	5.29358700	1.32143100	-2.12615800
C	8.62245800	2.47045100	-0.48133000
H	7.41189200	2.90010500	1.26701400
C	6.28273200	0.07562000	3.66002300
H	4.59102500	0.60999900	2.47597500

C	7.78348900	-1.54384900	2.72269400
S	7.37023400	-2.97253700	0.44800200
C	6.94369100	-2.94459300	-2.24015600
H	3.90575700	-0.56777600	-2.16912800
C	5.14981300	-1.82353500	-3.37397900
C	8.61507300	2.00152700	-1.80377000
H	7.40687600	1.23057800	-3.42456000
H	9.55591100	2.78887000	-0.02127800
C	7.44754400	-0.68220300	3.77037900
H	5.97277600	0.73623100	4.46696600
H	8.66867000	-2.17413300	2.79021200
C	6.25320600	-2.67624900	-3.42466400
H	7.80327000	-3.61285000	-2.24327800
H	4.57948900	-1.60137400	-4.27367100
H	9.54414200	1.95854200	-2.36960300
H	8.07648700	-0.62173600	4.65530000
H	6.56942100	-3.13155100	-4.36018000

References

(1) Fulmer, G. R.; Miller, A. J. M.; Sherden, N. H.; Gottlieb, H. E.; Nudelman, A.; Stoltz, B. M.; Bercaw, J. E.; Goldberg, K. I. NMR Chemical Shifts of Trace Impurities: Common Laboratory Solvents, Organics, and Gases in Deuterated Solvents Relevant to the Organometallic Chemist. *Organometallics* **2010**, *29* (9), 2176–2179.

(2) Emslie, D. J. H.; Blackwell, J. M.; Britten, J. F.; Harrington, L. E. A Zwitterionic Palladium(II) H3-Boratoxypentadienyl Complex: Cooperative Activation of Dibenzylideneacetone between Palladium and a Phosphine/Thioether/Borane Ligand. *Organometallics*, **2006**, *25* (10), 2412–2414.

(3) dos Santos, P. L.; Ward, J. S.; Data, P.; Batsanov, A. S.; Bryce, M. R.; Dias, F. B.; Monkman, A. P. Engineering the Singlet-Triplet Energy Splitting in a TADF Molecule. *J. Mater. Chem. C* **2016**, *4* (17), 3815–3824.

(4) Kukhta, N. A.; Batsanov, A. S.; Bryce, M. R.; Monkman, A. P. Importance of Chromophore Rigidity on the Efficiency of Blue Thermally Activated Delayed Fluorescence Emitters. *J. Phys. Chem. C* **2018**, *122* (50), 28564–28575.

(5) Allan, D. R.; Nowell, H.; Barnett, S. A.; Warren, M. R.; Wilcox, A.; Christensen, J.; Saunders, L. K.; Peach, A.; Hooper, M. T.; Zaja, L.; et al. A Novel Dual Air-Bearing Fixed-χ Diffractometer for Small-Molecule Single-Crystal X-Ray Diffraction on Beamline I19 at Diamond Light Source. *Crystals* **2017**, *7* (11), 336.

(6) Johnson, N.; Waddell, P.; Clegg, W.; Probert, M.; Johnson, N. T.; Waddell, P. G.; Clegg, W.; Probert, M. R. Remote Access Revolution: Chemical Crystallographers Enter a New Era at Diamond Light Source Beamline I19. *Crystals* **2017**, *7* (12), 360.

(7) Krause, L.; Herbst-Irmer, R.; Sheldrick, G. M.; Stalke, D. Comparison of Silver and Molybdenum Microfocus X-Ray Sources for Single-Crystal Structure Determination. *J. Appl. Crystallogr.* **2015**, *48* (1), 3–10.

(8) Sheldrick, G. M. A Short History of *SHELX*. *Acta Crystallogr. Sect. A Found. Crystallogr.* **2008**, *64* (1), 112–122.

(9) Sheldrick, G. M. Crystal Structure Refinement with *SHELXL*. *Acta Crystallogr. Sect. C Struct. Chem.* **2015**, *71* (1), 3–8.

(10) Sheldrick, G. M. *SHELXT* – Integrated Space-Group and Crystal-Structure Determination. *Acta Crystallogr. Sect. A Found. Adv.* **2015**, *71* (1), 3–8.

(11) Dolomanov, O. V.; Bourhis, L. J.; Gildea, R. J.; Howard, J. A. K.; Puschmann, H. *OLEX2* : A Complete Structure Solution, Refinement and Analysis Program. *J. Appl. Crystallogr.* **2009**, *42* (2), 339–341.

(12) Pander, P.; Data, P.; Dias, F. B. Time-Resolved Photophysical Characterization of Triplet-Harvesting Organic Compounds at an Oxygen-Free Environment Using an iCCD Camera. *J. Vis. Exp.* **2018**, *142*, e56614.

(13) Rothe, C.; Monkman, A. P. Triplet Exciton Migration in a Conjugated Polyfluorene. *Phys. Rev. B - Condens. Matter Mater. Phys.* **2003**, *68* (7), 075208.

(14) Cardona, C. M.; Li, W.; Kaifer, A. E.; Stockdale, D.; Bazan, G. C. Electrochemical Considerations for Determining Absolute Frontier Orbital Energy Levels of Conjugated Polymers for Solar Cell Applications. *Adv. Mater.* **2011**, *23* (20), 2367–2371.

(15) Data, P.; Motyka, R.; Lapkowski, M.; Suwinski, J.; Monkman, A. P. Spectroelectrochemical Analysis of Charge Carriers as a Way of Improving Poly(p-Phenylene)-Based Electrochromic Windows. *J. Phys. Chem. C* **2015**, *119* (34), 20188–20200.